Two-phase frictional pressure drop with pure refrigerant in vertical mini/micro channels

M.Sc. Thesis by

Muhammad Shujaat Ali

2018(S)-MS-TFE-4

Supervised by

Dr. Zahid Anwar

DEPARTMENT OF MECHANICAL ENGINEERING,NEW CAMPUS
UNIVERSITY OF ENGINEERING ANDTECHNOLOGY, LAHORE
JUNE 2020

Abstract:-

Conventionally used synthetic refrigerants (Chlorofluorocarbons, Hydro chlorofluorocarbons etc.) are considered to have significant impact on environmental degradation owing due to their high ozone depletion potential and global warming potential. Global treaties (Kyoto protocol) are now coming into force and asks for ban on utilization of potential harmful fluids. Refrigeration and air conditioning industry is therefore in search of environmental benign alternatives.

With growing quest on optimum utilization of energy sources devices used for exchange of thermal energy are now becoming more compact while required thermal duty is increasing day by day. Phase change heat transfer process in compact channels is now becoming increasing popular due to its capability to withstand high heating/cooling loads. Pressure drop is an important parameter and in case of phase change process this may affect system's thermal performance. Accurate estimation of pressure drop and its proper consideration in the design process is crucial to assure functionality of any thermofluid system involving phase change heat transfer process.

The current research is therefore emphasized on frictional pressure drop during flow boiling of environmental benign refrigerants (GWP<150), isobutane, HFC-152a, HFO-1234yf were tested against commonly deployed HFC-134a. The data presented here was collected under heat flux controlled conditions, the test piece was a round tube (L_{heated}=245 mm) while experimentation was performed at 27 and 32°C with mass velocity in 50-500 kg/m²s range. The effects of key parameters like heat flux, mass velocity, exit quality, operating medium were critically analyzed. It was observed that pressure drop increases as mass velocity increases in the test piece, increases with increase in exit vapor quality while the same was noticed to decrease with an increase in operating saturation temperature. Parametric effects and prediction assessment of correlations is reported.

Acknowledgment:-

Table of Content

Nomenclature:

A_c	Cross sectional area [m^2]
A_h	Heat surface area [m^2]
C_p	Specific heat capacity [J/kg.k]
d	Hydraulic diameter of the channel [m]
f	Friction factor [-]
F	Convective boiling enhancement factor [-]
g	Gravitational acceleration [m/s^2]
G	Mass Flux [$kg/m^2 s$]
I	Current supplied [A]
K	Thermal conductivity [w/mk]
L_{heated}	Heated length of test section [m]
$\dot{m}$	Mass flow rate [kg/s]
P	Pressure [bar]
P_r	Reduced pressure [-]
q''	Heat flux [kW/m^2]
R_a	Average roughness value [μm]
S	Nucleate boiling suppression factor [-]
t	Temperature [°C]
v	Specific volume [m^3/kg]
V	Voltage [V]
x	Vapor quality [-]
z	Axial location [m]
z_o	Sub cooled/Single phase length [m]
Δp	Pressure drop [mbar]

Greek letters

α	Heat transfer coefficient[$kW/m^2 K$]
σ	Surface Tension [N/m]

ρ	Density [kg/m^3]
μ	Dynamic viscosity [N.s/m^2]

Subscripts

Wall,z	Wall on location z
Tp	Two-phase flow conditions
t_{sat}	Saturation temperature
l_o	Liquid only
f_{fl}	Fluid surface parameter
Nb	Nucleate boiling
Turb	Turbulent flow conditions
Sat	Saturation condition
Fluid,z	Fluid at location z
l_{am}	Laminar flow condition
CHF	Critical heat flux
GWP	Global warming potential
ODP	Ozone depletion potential
MAE	Mean absolute error $MBE = \frac{1}{N}\sum_{i=1}^{N}\left(\frac{x_{predicted,i} - x_{experimentaion,i}}{x_{experimentaion,i}}\right) * 100\%$
HFC	Hydro-fluorocarbon

Dimensionless Group

Eo	Eotovs No.	$\left[\frac{(\rho_l - \rho_g)gd^2}{8\sigma}\right]$
Co	Confinement No	$\sqrt{\frac{\sigma}{g(\rho_l - \rho_g)d^2}}$
Bo	Bond No	$\left[\frac{q''}{G.h.l.g}\right]$
Nu	Nusselt No	$\left[\frac{h.d}{k}\right]$
Pr	Prandtl No	$\left[\frac{\mu.C_P}{K}\right]$
We	Weber No	$\left[\frac{G.d}{\mu.\rho}\right]$
Re	Reynold No	$\left[\frac{G.d}{\mu}\right]$

List of Figures:

List of Tables:

Chapter 1 Introduction

1.1 Background Information

Heat exchange is a vital process in various power and process-related applications namely power plants, automotive, nuclear reactors, electronic chips and so on. Modern compact high tech chips generate huge amount of heat (heat flux: heat dissipation rate per unit area kW/m^2) and need smart cooling solutions to ensure their effective operation. Enhancement of surface area and velocity of flowing medium along with manipulation of transport properties of the working medium are common options available for increasing/intensifying the heat exchange process. The frictional pressure drop is another critical parameter that affects fluid flow process, it also helps designers to choose the right operating conditions and equipment that can sustain required fluid flow. An accurate estimate of frictional pressure drop is, therefore, a key requirement while designing any device involving fluid flow for the exchange of thermal energy.

Recently compact devices are becoming popular to cope with effective space utilization. Within the heat transfer field also utilization of compact channels (d<3mm) is increasing, such channels offer a significant increase in surface area per unit volume of fluid flowing through them and are supposed to have better thermal performance compared with their conventional counterparts (d>3mm) [1]. Utilization of such compact channels and devices designed with them also helps in reducing the required material and fluid charge, additionally speculated improved thermal performance offers possibility/capability to withstand high heat flux. Two-phase (boiling/condensation) flow conditions capitalizing on fluid's latent heat of vaporization further help in improving the capability to withstand high heat flux and control of local hot spots. High heat fluxes (>100 kW/m^2) can be transferred over a quite small temperature lifts with devices made with compact channels and experiencing two-phase flow conditions [2]. As channel size shrinks friction associated with fluid flow through the channel also increases, this translates into increased pumping power for sustaining fluid flow through the system [3-4].

Literature review revealed that a significant proportion of energy in built environment is being consumed by air conditioning equipment. In addition, indoor conditions (especially temperature, humidity, odor, etc.) have a remarkable effect on work performance. Conventionally synthetic refrigerants are used to run these devices, such mediums if leaked from the system may have considerable environmental footprint due to their high levels of global warming and ozone depletion potentials (GWPs & ODPs) [5].

Growing environmental awareness and strict legislation asks for replacement of existing refrigerants either with natural ones or with synthetic refrigerants with low GWP and ODP levels [6-7]. Literature review shows limited information for low GWP compounds with a focus on thermal dissipation and pressure drop aspects, therefore there is a need to test different potential alternative candidates under wide operating conditions so that efficient operating conditions and devices can be designed identified for coping ever-growing energy dissipation demands [8].

Legislative institutions all over the world are trying to mitigate the refrigerant risks by applying strict agreements such as climate agreement, the EU F-gas Regulation [9]. The Kyoto Protocol's objective was to reduce carbon emission by diminishing greenhouse gas emissions. The goals of the main contribution period of the Kyoto Protocol include the outflow of six primary greenhouse gases, HFCs, CO_2, CH_4, NO_2, PFCs and SF_6 [10-11]. Although the literature on phase-change heat transfer has been widely discussed and reported in literature, the general understanding is still limited specially for transport process in narrow channels. Therefore, further experimental work still needs to be done using reliable equipment and under broad operating conditions/parameters, this will help in improving current understanding and unveiling hidden physics. The work reported here was therefore conducted with environment bengin mediums where three natural and synthetics mediums were tested for their frictional pressure drop during flow boiling in a vertical mini channel. The results were compared with conventionally used R-123a. Details discussion on parametric effects and assessment of prediction methods were the key objective of the study.

1.2 Defining Mini/Microchannel:

A channel is used for two purposes: (1) liquid interaction with walls and (2) bring new fluid to the walls and take away fluid from the enclosure while the transport is carried out. Engineering

community is not yet on consensus for defining transition criteria about channel sizes. Commonly cited definitions are summarized below [12]

Kandlikar and Grande [13] used nominal diameter of the channel as defining parameter, they considered channels with d<3 mm as mini channel while the rest were considered to be macro channels. In his work Mehendale et al. [14] identified presence of mesoscale in between micro and macroscales as reported by Kandlikar and Grande [15]. The channels falling in mesoscale has their characteristic dimension in 100-1000 µm range. The above stated two definitions are tabulated in Table **1-1**.

Table 1-1: Limits for channel transition

Channel	Mehendale et al. [14]	Kandlikar & Grande [15]
Micro-channel	d 1-100 µm	d 10-200 µm
Meso-channel	d 100-1000 µm	-----------------
Mini-channel	-----------------	d 200 µm- 3mm
Macro-channel	d 1-6 mm	-------------------
Conventional channel	d > 6mm	d >3 mm

Figure 1.1 shows the ranges of channel dimensions employed in various systems. From an engineering standpoint, there has been a steady shift from larger diameters, on the order of 10–20 mm, to smaller diameter channels. Since the dimensions of interest are in the range of a few tens or hundreds of micrometers, usage of the term "microscale" has become an accepted classifier for science and engineering associated with processes at this scale [12].
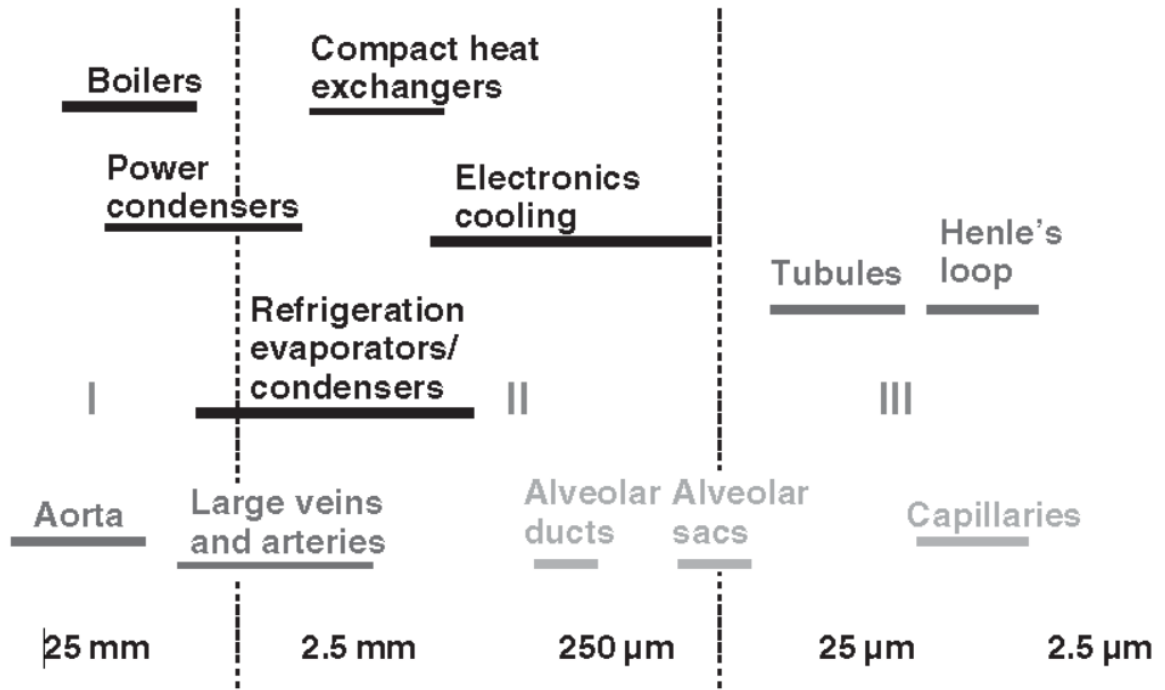
Figure 1.1: Range of channel diameter employed in various applications [12]

Boiling process is characterized by generation of vapor bubbles during heating process, technically if development of bubble is restricted with channel size than channel can be considered as mini/micro channel. Definitions based on these criteria are summarized below,

The confinement in mini/micro-channel prevents the development of the bubble in a radial direction. In order to take account of this restriction, Kew and Cornwell [16] suggested the confinement number (Co). They reported remarkable confinement consequences for cases where Co > 0.5, where Confinement number was defined by in Eq.(**1-1**);

$$C_o = \frac{\sqrt{\dfrac{\sigma}{g\left(\rho_l - \rho_g\right)}}}{d} \tag{1-1}$$

Confinement consequences are important for channels with Co >1 according to the guidelines of Triplet et al.[17]. Ong and Thome [18] recommended a changeover from macro to micro scale within the assortment of Co 0.3-1 and called this conversion meso-scale, while micro-scale consequences have been reported for Co >1. Harirchian and Garimella [19] introduced another dimensional-less parameter to differentiate between micro and macro-conduits called the convective confinement number. The authors found the flow velocity to be an integral factor to change from macro to micro-scale limit. This criterion was based on their experimental findings with FC-77 and is summarized as follows Eq.(**1**-**2**):

$$\text{Bd}^{0.5} < Re \ 160 \ (\text{for microchannel}) \tag{1-2}$$

Li and Wu [20] suggested the following dimensionless criteria, reflecting on the relative significance of viscous, surface stress, and pseudo forces.

$$\text{Bd} * \text{Re}^{.5} < 200 \ (\text{For micro} - \text{channel}) \tag{1-3}$$

Ullman and Brauner provided another term based on Eötvös Numer (Eo). This principle is also focused on containment of bubbles and relates buoyancy and surface tension forces:

$$\text{Eo} < 1.6 \ (\text{For micro} - \text{channel}) \tag{1-4}$$

1.3 Introduction to Boiling:

Visually boiling process is evidenced by generation of vapor bubbles in stationary or flowing fluid, this is an endothermic reaction and needs supplement of heat for its execution in real life. Boiling may occur under free and forced convection phenomena, and classified into sub-cooled and saturated boiling. In case of sub-cooled boiling, the bulk temperature of a fluid is lower than

14

the saturation temperature and air pockets developed. In saturated boiling, the liquid temperature equal than saturation temperature bubbles were formed and pushed by buoyancy forces through the liquid, ultimately fleeing from a free surface.

Different operating regimes during boiling process are graphically clarified via drawing a boiling curve, it shows the change in the value of heat flux plotted against degree of wall superheat (schematically presented in Figure **1**.**2**). Case shown in Figure **1**.**2** is not drawn as per scale and refers to pool boiling situation however similar regimes does exist according to flow boiling. Actual diagram may vary based on the related fluid parameters and working conditions.

There are four major portions of the boiling curve that can be seen in Figure **1**.**2**. First is the zone of the natural convection region (o-a). This zone thermal dissipation/heat transfer is caused by conventional current as surface and fluid temperatures are a little higher than saturation state. The nucleation status of bubbles in this zone is not fully addressed. The second region is nucleate boiling (a-c) in which two portions exist. In the first region bubbles are produced while in the second region, bubbles move upward and form a film. Bubble nucleation begins with the gas vapors present in the surface cracks and these bubbles collapse into vapor slugs and increases the fluid circulation around them, thereby achieving better heat transfer. During the analysis of heat flux applications, the external temperature increases rapidly in c-e, over steps in the central point. Point "c" represent the maximum value of heat flux (CHF) and it can also be explained as a point of moving away from a nucleate boiling point. While the surface temperature increases, physical burnout may take place this phenomenon is also recognized as burnout heat flux.
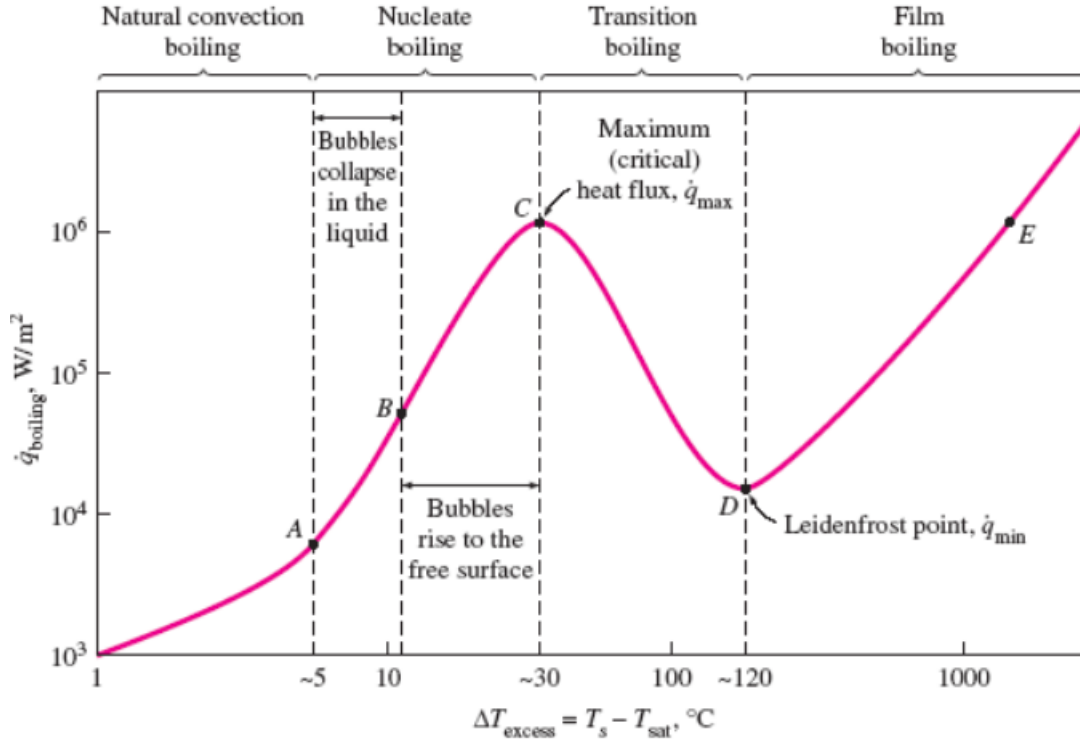
Figure 1.2: Typical boiling curve for pool boiling [21]

The third portion is transition region (c-d) where heated outer surface quickly transforms from wet to dry state. The fourth region is the film boiling zone (d-e), where the heated surface is coated with a constant layer of vapor. The lowest point of film boiling named Ledienfrost point [21].

A subcooled liquid flow entering a vertical and uniformly heated tube with a known heat flux over its length can be considered as one of the simplest scenarios of forced convective boiling in a tube and is ideal for illustration purposes. For a given heat flux and mass flow rate the liquid eventually will evaporate completely provided the tube is long enough. Flow regimes encountered over the length of heated tube are shown in Figure **1.3**, specifically for the vertical flow orientation. The picture illustrates the temperature different and corresponding heat transfer regions.

Region A (single-phase convection): When the liquid enters the heated tube the temperature increases gradually up to the saturation temperature, while the wall temperature remains below the temperature required for nucleate boiling. For this condition the heat transfer to the liquid is a single-phase convective heat transfer only.

Region B (subcooled nucleate boiling region): At a certain length along the tube, the formation of vapour bubbles start to occur at the wall which is now superheated (ΔT_{sat}>0) even though the bulk liquid may still be in a subcooled state (ΔT_{sub} >0) [29]. Bubbles form, grow and detach from the heated surface and collapse in the subcooled bulk flow and this defines the first part (B) of the bubbly flow regime.

Region C (saturated nucleate boiling region): In this region the liquid reaches the saturation temperature and the transition between regions B and C is the point at which the thermodynamic quality is such that x=0. Bubbles grow and detach from the surface and are entrained into the bulk flow. This is the second part C of the bubbly regime.

Regions D and E (the two-phase forced convective region of heat transfer): As the quality increases, a point may be reached where the mechanism of heat transfer changes from a process of "pure boiling" to a process which includes "evaporation", and the flow pattern changes from bubbly or slug and churn flow to annular flow.

Regions F: In this region, the low thermal resistance of the thin liquid film may become sufficient to prevent the liquid, in contact with the wall, to be superheated to a temperature that allows bubble nucleation. This means the heat is removed more effectively from the wall by forced convection toward the liquid-vapour interface, which causes liquid to evaporate, without nucleation occurring.

Region G (liquid deficient region): When the liquid film evaporates completely, this called the critical heat flux (CHF) or dryout condition, and is accompanied by a rise in the wall temperature. For a constant heat flux, this condition may cause extreme wall temperature levels and is typically avoided in heat exchanger designs.
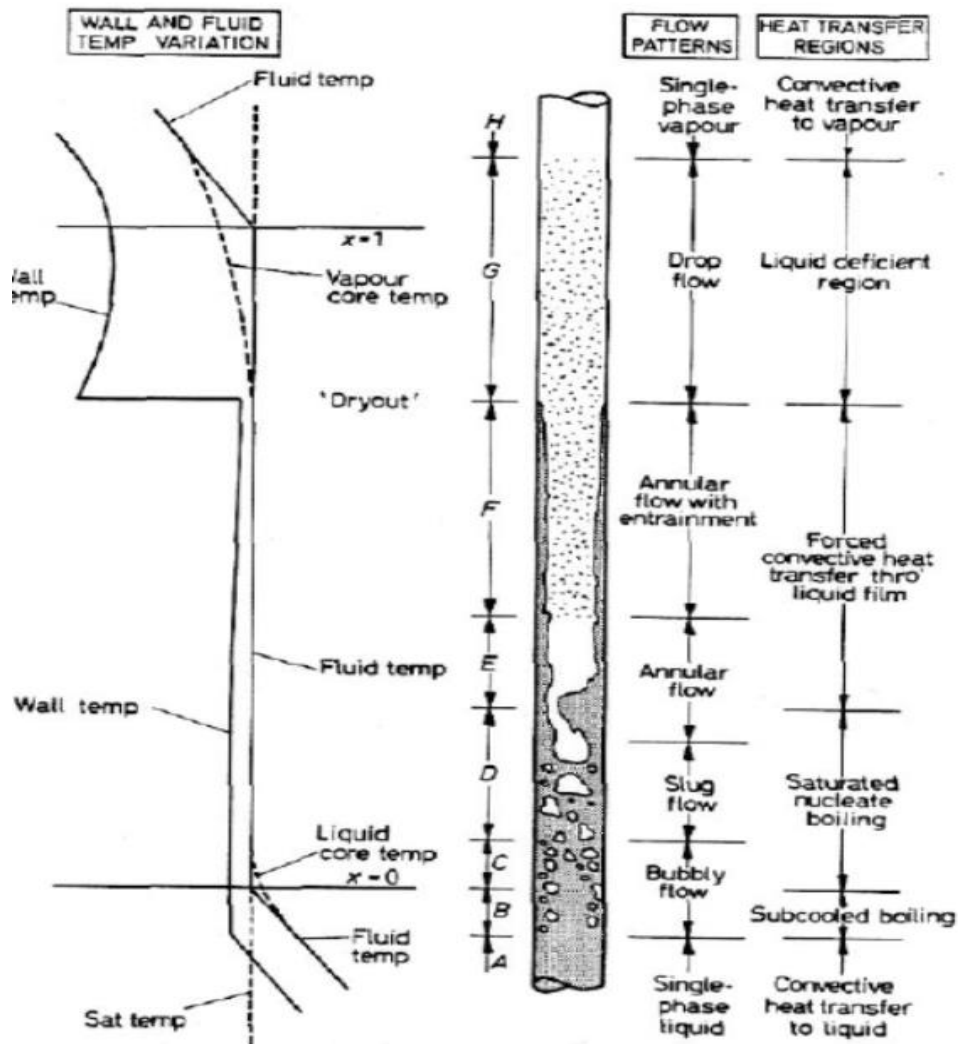
Figure 1.3: Flow regimes for forced convection boiling in a vertical tube [22]

1.4 Introduction to pressure drop:

Pressure drop is characterized as the difference between two points of a liquid transport system in the total pressure. Pressure drop occurs when flow resistance forces allow the fluid to pass through the conduit. The fluid flow resistance depends on the fluid velocity through the pipeline. Industrial engineers must account for pressure drop. Pressure drop is a sign of frictional forces that are present in a piping system. With increasing the pressure drops, machine pumps often

raise the power required to account for this, leading to greater operating cast. Therefore, the frictional pressure drop is an essential factor that may affect the fluid flow process and it also helps in choosing the right operating conditions and equipment to manage the fluid flow necessary.

In the modern industry, two-phase flow is widely applied. We may mention the massive use of refrigeration, air conditioning, food and petroleum processing which has widespread use for two-phase flows. The majority of applications need accurate prediction in order to design the components such as pumps and pipelines for two-phase frictional pressure drop and it has been combined with elements of frictional, acceleration, and gravitational.

The simplest approach to the prediction of two-phase flows is to treat the entire two-phase flow as if it were all liquid. The two-phase pressure drops for flows inside pipes and channels are the sum of three contributions:

- the static pressure drop $\Delta \mathbf{p_{static}}$ (<u>elevation head</u>)
- the momentum pressure drop $\Delta \mathbf{p_{mom}}$ (<u>fluid acceleration</u>)
- the frictional pressure drop $\Delta \mathbf{p_{frict}}$

The total pressure drop of the two-phase flow is then:

$$\Delta P_{total} = \Delta P_{static} + \Delta P_{mom} + \Delta P_{frict} \qquad (1\text{-}5)$$

The static and momentum pressure drops can be calculated similarly as in case of single-phase flow and using the homogeneous mixture density:

$$\rho_m = \alpha \rho_v + (1 + \alpha)\rho_l \qquad (1\text{-}6)$$

The most problematic term is the frictional pressure drop Δp_{frict}, which is based on the single-phase pressure drop that is multiplied by the two-phase correction factor (homogeneous friction multiplier – Φ_{lo}^2). By this approach the frictional component of the two-phase pressure drop is:

$$\left(\frac{dp}{dz}\right)^{2f} = \square_{lo}^{2f}\left(\frac{dp}{dz}\right)^{f} \tag{1-7}$$

where $\left(\frac{dp}{dz}\right)^{2f}$ is frictional pressure gradient of two-phase flow and $\left(\frac{dp}{dz}\right)^{f}$ is frictional pressure gradient if entire flow flows as liquid in the channel (standard single-phase pressure drop). The term Φ_{lo}^{2} is the homogeneous friction multiplier that can be derived according to various methods. One of possible multipliers is equal to $\Phi_{lo}^{2} = \left[1 + x_g\left(\frac{\rho l}{\rho g} - 1\right)\right]$ and therefore:

$$\left(\frac{dp}{dz}\right)^{2f} = \left[1 + x_g\left(\frac{\rho l}{\rho g} - 1\right)\right]\left(\frac{dp}{dz}\right)^{f} \tag{1-8}$$

An alternate approach to calculate two-phase pressure drop is the separated-phases model. In this model, the phases are considered to be flowing separately in the channel, each occupying a given fraction of the channel cross section and each with a given velocity. It is obvious the predicting of the void fraction is very important for these methods. Numerous methods are available for predicting the void fraction.

The method of Lockhart and Martinelli is the original method that predicted the two-phase frictional pressure drop based on a friction multiplicator for the liquid-phase, or the vapor-phase:

$$\Delta p_{frict} = \emptyset_{ltt}^{2}\Delta p_l(\text{Liquid} - \text{phase }\Delta p) \tag{1-9}$$

$$\Delta p_{frict} = \emptyset_{gtt}^{2}\Delta p_g(\text{vapor} - \text{phase }\Delta p) \tag{1-10}$$

The two-phase multipliers Φ_{ltt}^{2} and Φ_{gtt}^{2} are equal to:

$$\emptyset_{ltt}^{2} = 1 + \frac{C}{X_{tt}} + \frac{1}{X_{tt}^{2}}, \text{for } Re_l > 4000 \tag{1-11}$$

$$\emptyset_{gtt}^2 = 1 + \frac{C}{X_{tt}} + \frac{1}{X_{tt}^2}, \text{ for } Re_l < 4000 \tag{1-12}$$

where X_{tt} is the Martinelli's parameter defined as:

$$X_{tt} = \left(\frac{1-x}{x}\right)^{0.9} \left(\frac{\rho_g}{\rho_l}\right)^{0.5} \left(\frac{\mu_l}{\mu_g}\right)^{0.1} \tag{1-13}$$

And the valve of C in these equations depends on the flow regimes of the liquid and vapor. These values are in the following table.

Table 1-2: Values of C for case of liquid and gas region

Liquid	Gas	C
Turbulent	Turbulent	20
Laminar	Turbulent	15
Turbulent	Laminar	10
Laminar	Laminar	5

1.5 Main Objectives:

The work reported in this study was undertaken with the ambition to improve understanding related with frictional pressure drop under flow boiling conditions. The whole work was divided into following tasks;

- Extensive literature review of the field with generation of a large databank (wide operating conditions for pure refrigerants in mini/micro channels) for saturated flow boiling from stable operating conditions.
- Parametric analysis to clarify role of key parameters (heat flux, mass flux, vapor quality, saturation temperature, channel geometry, etc.).
- Evaluation of prediction methods and development of a generalized reliable correlation

The findings could be beneficial for the structure of portable heat exchangers for the cooling, heat pump and smart coiling industries.

1.6 Structure of the thesis:

The first chapter covers the introduction, history, and fundamental rules of the boiling process. Literature review of current research is addressed in Chapter 2. The details of the experimental setup, instrumentation and a procedure for data analysis are described in chapter 3. Experimental results of two-phase frictional pressure drop are reported in chapter 4. Chapter 5 describes the results of the study as well as possible future suggestions.

Chapter 2 Literature Review

Mini/micro channel is being used in a extensive range of applications including but not limited to cooling of electronics, compact heat exchangers, automotive, etc [23]. The literature surge revealed enormous data about heat dissipation and liquid flow characteristics in compact channels. Although many studies exist in the literature about pressure drop recorded with a variety of mediums and operating conditions but contradictory trends have been noticed from the literature review exercise.

This chapter summarizes experimental findings from the literature review, keeping in view recent legislation, attention was focused on environment friendly alternatives (GWP<150).

2.1 Frictional Pressure Drop:

Operating pressure is one of the factors that may have an impact on overall thermal performance for a two-phase system, therefore accurate assessment of frictional pressure drop and its proper account should be exercised while selecting operating conditions [24], [25]. While channel confinement may potentially increase heat transfer performance this will also increase pressure drop (will require more pumping power).

During experimental campaigns, pressure sensors were used to monitor the pressure drop across the experimental conduit. It was recorded from the measurement device that from a various aspects including gravity, acceleration, friction and other related matters. The change in pressure was measured in the annular flow region and the gravity consequence was corresponding to the difference of shear stress at the liquid film's surface. Viscosity can be understood as friction between fluid molecules and it is the main influencing parameter on major friction losses in a straight channel ignoring the behavior of flow whether laminar or turbulent. Shear stress is produced between the fluid molecules and surface of the conduit and it produces friction loss.

Kim and Mudawar [26] documented a standard procedure for calculating a two-phase frictional pressure drop in mini/micro-conduit. The database consists of 9 running fluids. The diameter of conduit ranged (0.349 to 5.35 mm), and the new technique offered an impressive representation of the entire system (17.2% MAE). It also showed predictive reliability by flowing numerous

operating fluids in single and multi-channels, mass velocity, quality and pressure both single and multi-channels.

The comparative flow behavior study of R152a, R134a, R1234z(E), and R1234yf in the fine inner walls of a 4 mm tube was conducted by Longo et al [27]. Three saturation temperature values from 30-40°C were selected to perform experiments by varying vapor content and mass velocity resulting in variation in pressure drop. Entire data of frictional pressure drop ~~data~~ was observed by Friedel [28], while Akers [29] provided a better approximation of the thermal coefficients of condensation. R152a, R1234yf and R1234z(E) demonstrated similar pressure drop and condensation heat dissipation performance of all refrigerants was observed analogous to R134a. Consequently, these refrigerants having low GWP appeared to be important long-term substitutes.

Lee and Pan [30] performed experiments to measure pressure drop in a tube (500 µm and 0.5 m long) carrying propane and compared their findings with well-known correlations of density and viscosity. Vapor quality was maintained between 0 and 1 while a mass flux range was selected from 360 to 915 kg/m^{2}s. A comparison of different models showed that Pamitran [31], Xuejiao, and Hibiki [32] used a separated type of model.

During the condensation of R152a, Liu et al. [33] identified experimental values for film coefficients and pressure drop in square and round micro-channels including different diameters (0.95 & 1.15 mm). Mass flux range was selected from 200-800 kg/m²s while saturation temperature values were kept at 40 and 50 °C during performance of experiments. The variation in pressure drop and heat dissipation was examined by different parameters. Both pressure drop and thermal efficiency exhibited a growing trend with a rise in mass flow and vapor quality whereas a decrease in their values was observed on increasing saturation temperature. For low mass fluxes, heat transfer was not affected by geometry to a greater extent but variation in pressure drop was observed.

Ewim & Meyer published experimental results on pressure drop in horizontal and inclined conduit having inner diameter was 8.37 mm [34]. The tests were performed at 40 °C varying mass flux from 50 to 100 kg/m²s. Two high-display–video cameras captured the flow pattern using optical lenses, at the start point and exit point of the test conduit. The effect of frictional

pressure drop was analyzed by changing vapor content, temperature, mass flux, and angle of inclination. It was observed that the pressure drop augmented with an escalation of mass flux and vapor content.

Hirose et al. [35] tested the pressure drop phenomenon in a micro fin conduit with 4 mm diameter. They investigated R32, R152a, and R410A for data analysis. For analysis of pressure drop and heat dissipation, mass flux varied from 100-400 kg/m²s at a 35 °C constant temperature. For the case of all refrigerants, approximately 1.6 times more value of frictional pressure drop was observed for mini duct as compared to a smooth one. The micro fin conduit's thermal efficiency was around about 2-7 times higher for R32 on maintaining velocity at 200 kg/m²s. The findings were compared with the predicted values for smooth and micro fin tubes and developed an innovative model.

Condensation of refrigerants in a horizontal conduit with mini-channels was reported by Jige et al. [36]. This research explored the pressure drop features on the various refrigerants in rectangular mini-channels. Mass velocity was maintained from 95 to 400 kg/m^{2}s and temperature was kept at 40 and 60 °C. The consequences of condensation characteristics were explained in terms of mass velocity, vapor content, temperature and the design of the rectangular conduit. In the case of horizontal rectangular mini-channels the proposed model successfully estimated the required properties.

Maqbool et al.[37] investigate pressure drop phenomenon in a conduit having a diameter 1.75 mm and a section of length 245 mm. Experiments were conducted at different temperatures and mass flow was from 95 to 600 kg/m^{2}s. They indicated that the frictional pressure drop augmented by escalating the mass flow, quality, and saturation temperatures. The findings of frictional pressure drop were in a close match against the well-predicted correlations (Müller-Steinhagen, Heck and Friedel).

Hossain et al. [38] established a two-phase frictional multiplier $(\emptyset_v)$ for pressure drop within a horizontal conduit. The test section consists of 3.6 m length and the experiment performed at different values of saturation temperature. The author investigated the outcome of mass velocity, configuration of channel, and surface tension. Existing correlation and the advanced phenomenon of a $(\emptyset_v)$ were analyzed to anticipate the condensation pressure drop of different

refrigerants within a horizontal conduit. The proposed correlation exposed improved performance for all refrigerants and was able to foresee experimental data within ±11%.

Xu and Fang [39] introduced a novel technique for a multiphase flow performance. The author compiled 530 data points of 9 different refrigerants from literature. The properties of compiled data were including diameter range from 0.2 to 11.05 mm. The previous models were analyzed against the experimental catalog. Depending on all experimental evidence a novel correlation with MARD 19.4% was planned.

Saisorn & Wongwises [40] examined the consequences of conduit diameter on the pressure change in the rounded micro conduit. Experiments were performed in different ranges of diameters (0.53, 0.22, and 0.15 mm) with different lengths (320, 120, and 110 mm) of conduits. The flow display was made easier by using the stereo zoom magnifying glass. The flow regimes graph developed from the identified flow trend and up to date model for the two-phase frictional multiplier was planned.

Chapter 3 Experimental setup

The information of test configuration and corresponding instruments are described in detail for the parameters of interest (vapor quality, mass flux, saturation temperature, etc).

In this study data was collected from a vertical test section which was placed in a closed-loop setup, tests were done with pure refrigerants. The setup was initially planned by Owhaib [41] and was promoted by Ali & Palm [3] and Maqbool et al [42] for their experimental campaigns with R134a, R245fa, Ammonia, and Propane. The data reported in this study was collected while operating with R134a, R152a, R1234yf, and R600a, for experimental campaign a different test section (d_i=1.60 mm, heated length=245 mm) was used in the aforementioned setup.

3.1 Methodology:

The proposed work will be started with data mining exercise; databank will be generated by digitizing data from published literature. The data will be critically analyzed for clarifying effect of operating medium, operating properties (heat flux, mass flux, vapor quality, operating pressure, operating medium, channel geometry and configuration). Finally statistical approach (multi variable based regression analysis with SPSS/EES or other spreadsheet based tools) will be used for development of new correlation.

Step wise methodology which will be adopted in order to complete this research is given blow.

   I.   Literature Review
  II.   Data Mining
 III.   Analysis of data collection
         i.   Parametric effects (mass flux, vapor quality, heat flux, saturation temperature, etc.)
        ii.   Assessment of correlation from literature
  IV.   Development of new correlation
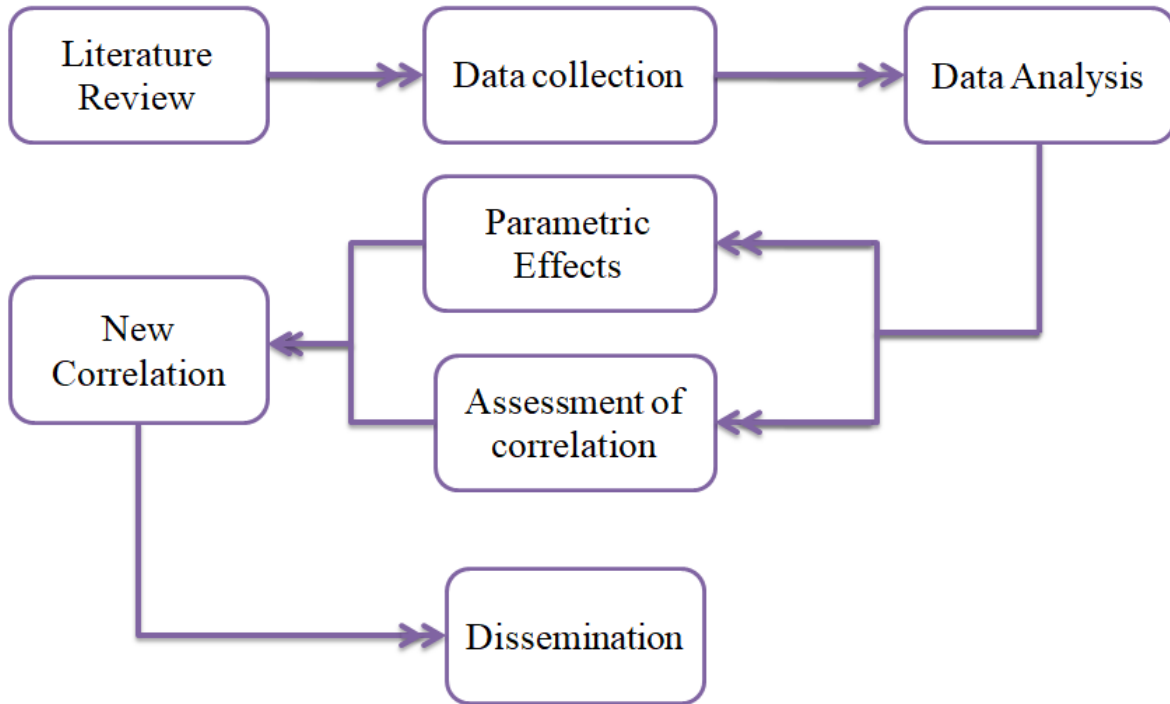   V.   Thesis writing

Figure 3.1: Flow diagram of M.Sc research

3.2 Experimental Setup:

A closed cycle method used in this experiment is shown in   Figure 3.2. The system has been equipped to automatically monitor cooling conditions, pressure, heat and mass flow level. Four natural refrigerants (R134a, R152a, R600a, and R1234yf) were monitored for fluid flow and pressure drop properties and tests were performed inside a small tube. In each case, conduit (d_i=1.06mm, d_o=2.0mm, l_h=245mm) was directly heated by DC power supply. A gear pump has been used for the process of fluid circulation. An absolute sort of pressure detector has been used to measure system pressure while a decrease in pressure before and after the conduit was recorded using a Druck PTX 5072. A coil was draped on the outer side of the conduit for preheating so that inlet conditions could be adjusted. In order to avoid the ingress of tiny grains, a 2 µm strainer has been installed prior to the test conduit. Thermocouples (copper/constantan) were placed on the external perimeter of the test area to monitor temperatures. The support of small container linked to the main cycle and managed to keep the temperature-controlled bath. The mass flow function has been controlled by varying the gear pump speed and calculating the mass flow by the inertial

mass flow meter (Coriolis mass flow meter). The tool that was attached to the computer name is a data logger and Aglient VEE has been used for the application of data capture.

3.3 Test Section:

In a metallic test conduit, fluid flow and pressure drop characteristics of four natural refrigerants were studied. Using DC electricity, the test conduit was heated. For the visual inspection of the beginning and ending of the conduit section the weight difference in the loaded and unloaded channel was used to determine the internal diameter of the conduit. For this calculation, an extremely precise scientific balance was utilized. The vacant conduit portion was balanced in the first stage and then replaced with purified liquid and estimated again. The inner diameter of its cylindrical duct was then assessed and performed this method various time and mean value was taken as the duct diameter.
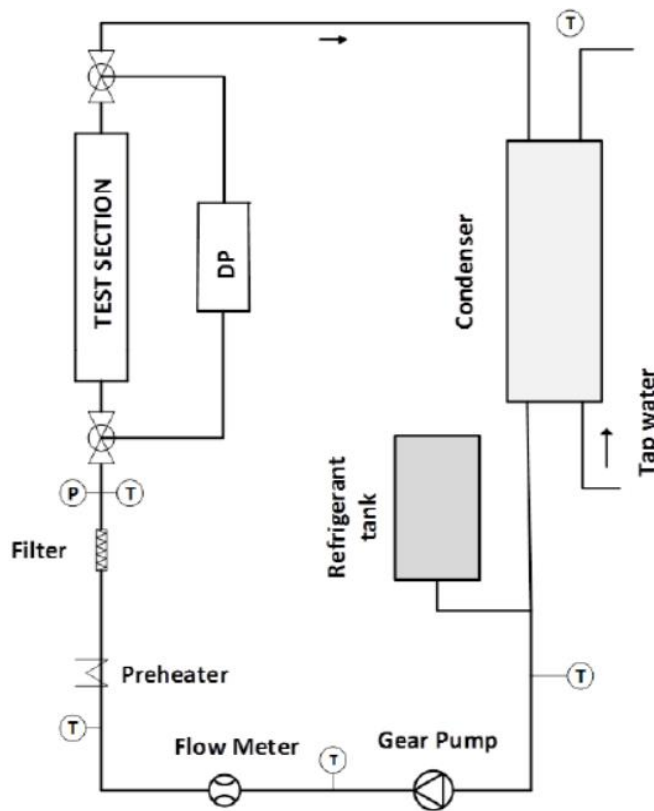
Figure 3.2: Block diagram of configuration [43]

For finding the wall temperature, used thermocouples at local positions (Figure 3.3). The roughness of the heating surface impacts the bubble nucleation process. This bubble nucleation process controls heat transfer performance. Talysurf PGI 800 scanned all the tubes to analyze the inner surface of a small channel. 0.95 µm was an average roughness value with maximum peak height was 2.69 µm and depth valley was 6.44 µm. Error! Reference source not found. shows the Conical stylus profilometry (roughness profile) of the heating surface.
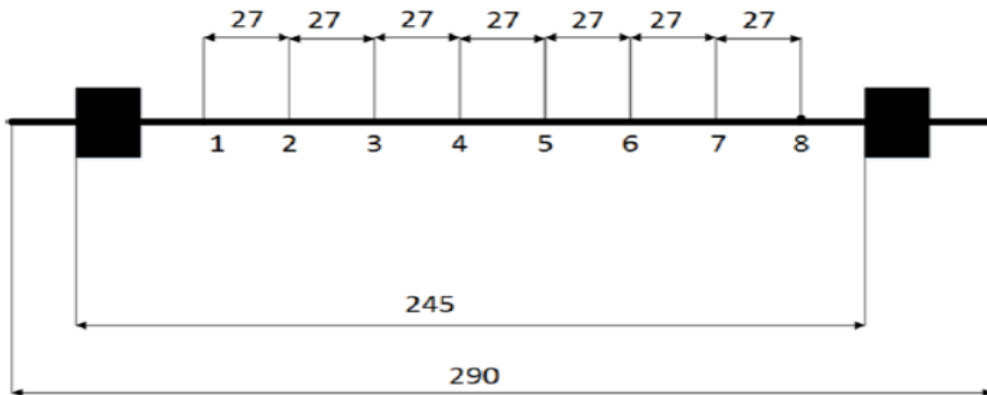
Figure 3.3: Position of thermocouple along the test section [44]
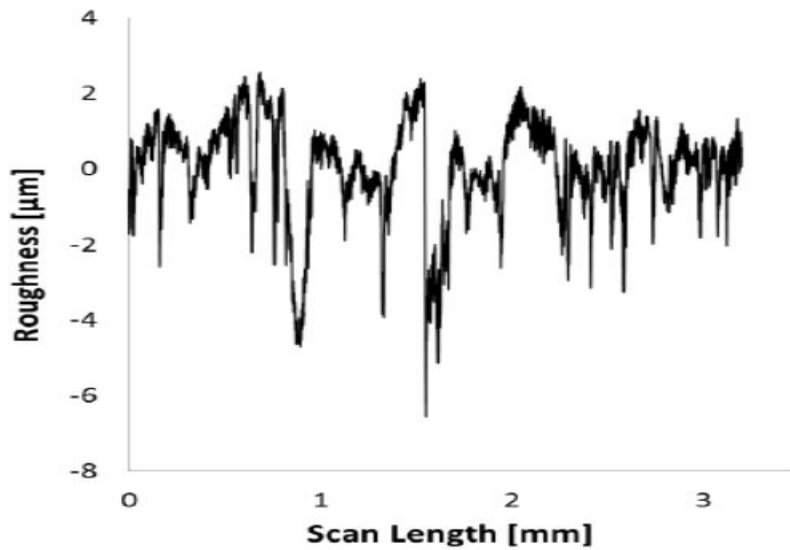
Figure 3.4: Conical stylus profilometry (roughness profile) of the heating surface [45]

Table 3-1: Roughness attributes of the heating surface

Parameter	Description	Formula	Value (µm)
R_a	Arithmetic average of absolute value	$R_a = 1/n \sum_{j=1}^{n} |Xj|$	0.95
R_v	Maximum Valley depth	$R_v = m_i n_j X_j$	6.44
R_p	Maximum peak height	$R_p = max_j X_j$	2.69

3.4 Data acquisition:
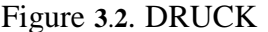
The signals of different instruments were analyzed and received by Agilent data longer (34970A). The data gathered for conditions of a stable state (apart from boiling and incipience and dry out conditions). The frequency of data gathering was within 0.3-0.5 Hz, and the data were assembled for almost 300 seconds. The median sample value was regarded as a nominal value of the data point. Engineering Equation Solver (EES) was used to measure refrigerant property data. Approximately 2% of the refrigerant property information considered ambiguity.

3.5 Measurement Instrumentation:

3.5.1 Temperature Measurements:

The highly sensitive thermocouples manufactured by Omega Engineering INC with positive and negative constantan wire were used for every temperature measurement in this study. The highly sensitive thermocouples (OMEGABOND 101) were mounted on the external surface of wall. Temperatures of the input and output fluids were determined using thermocouples made from stainless steel (TMQSS-020U-12 from Omega). The systematic failure was less than 0.001°C due to voltage-to-temperature transformations, while the error was 0.024°C (Agilent Technology) due to data longer resolution.

3.5.2 Pressure Measurements:

A high-performance absolute pressure transuding system from the Druck GE Crop was designed for the test device. As specified by the manufacturer, the precision of the system is 0.04 percent of the full value, including nonlinearity, hysteresis, and repeatable effects. The sensor has been placed between the preheater and the test area, shown in   Figure **3.2**. DRUCK DPI 603 configured both pressure transducers regularly to validate their reliability over the trial section. Consequently, moderate uncertainty figures were ±1 mbar in differential pressure measurements and ±10 mbar in absolute pressure.

3.5.3 Mass Flow Measurements:

For calculating the refrigerant mass flow rate a inertial flow meter (Coriolis mass flow meter) has been used. The change in flow rate was 0.2-1 g/s during the trial period of this study. The flow meter performance improved as the flow rate increased (Figure **3.5**). A consecutive calculation of the overall uncertainty was, therefore, ±3%.

3.5.4 Input Power Measurements:

For heating the sample conduit have been performed by Manson SPS-9600. The input of the test conduit was calculated through the combination of current intensity and voltage drop. The

specified power supply was ± (1% +1 count). For separate and accurate voltage calculation, a precise digital voltmeter was used.
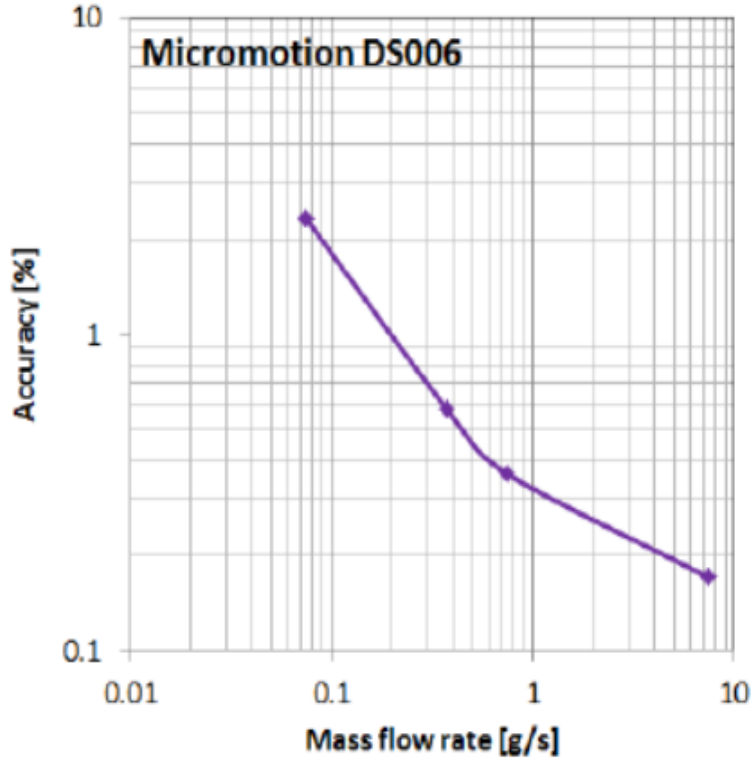
Figure 3.5: Efficiency of a mass meter [44]

3.6 Data reduction for Two-Phase flow:

The local thermal dissipation factor was estimated.

$$\alpha_z = \frac{q^{''}}{t_{\text{wall in,z}} - t_{\text{sat,z}}}$$

(3-1)

$t_{\text{sat,z}}$ and $t_{\text{wall in,z}}$ represent the local and inner wall temperature at position z respectively. The local temperature was measured using entrance pressure and pressure drop throughout the test segment. For pressure drop, a linear pattern was regarded throughout the test conduit. Input and heat were applied to the fluid to measure the value of the vapor in every position as follows:

$$x_z = \frac{\pi(z - z_o)q''d}{A_c h_{lg} G} \tag{3-2}$$

A_c and z_o is the destination where saturated situations have been identified as:

$$z_o = \frac{m \cdot C_p(t_{sat} - t_{in})}{dq''\pi} \tag{3-3}$$

The pressure drop calculated by the differential pressure sensor incorporates the contribution of single-stage, two-phase and pressure drop due to trivial loses (inlet, outlet, etc.).

$$\Delta p_{measured} = \Delta p_{single\ phase} + \Delta p_{minor\ loss} + \Delta p_{two-phase} \tag{3-4}$$

$\Delta p_{two-phase}$ is the mixture of acceleration, frictional and gravitational influences.

$$\Delta p_{two-phase} = \Delta p_{gravitational} + \Delta p_{acceleration} + \Delta p_{frictional} \tag{3-5}$$

Chapter 4 Experimental results of two-phase frictional pressure drop:

Frictional pressure drop is a crucial factor that will helpful for picking the right components and pumps for any physical implementation and also helpful in designing the compact heat exchanger, modern high technology application requires smart cooling [46]. Table **4-1** provides a comprehensive description of the working situations for a two-phase frictional pressure drop.

Table 4-1: Comprehensive description of working conditions

Refrigerants	Diameter [mm]	Heated length [mm]	Saturation temperature [°C]	Mass Flux [kg/ms^2]	$\Delta t_{sub,in}$ [K]	x [-]	Ra [µm]
R1234yf	1.60	245	27,32	50-500	1-1.5	Until dryout	0.95
R134a	1.60	245	27,32	50-500	1-1.5	Until dryout	0.95
R152a	1.60	245	27,32	50-500	1-1.5	Until dryout	0.95
R600a	1.60	245	27,32	50-500	1-1.5	Until dryout	0.95

Differential pressure sensors used to detect the pressure drop of multiple effects as mentioned in Eq.(4-1). The pressure drop at the ends and the single-phase pressure drop was described in accordance with the standard methodology explained by Maqbool [47]. The dp$_{tp}$ has been determined with subtraction from the estimated pressure drop of all other contribution (4-2).

$$dp_{measured} = dp_{sp} + dp_{end\ effects} + dp_{tp} \qquad (4\text{-}1)$$

$$\mathbf{dp_{tp} = dp_{acceleration} + dp_{frictional} + dp_{gravitational}} \qquad (4\text{-}2)$$

The explanation for gravitational pressure drop is to the location of conduit and it's measured as:

$$\left(\frac{dp}{dz}\right)_{gravitational} = \sin\emptyset\left[\rho_l(1-\alpha) + \alpha\rho_g\right]$$

(4-3)

According to the homogenous model, α is the void fraction

$$\alpha = \left[1 + \left(\frac{\rho_g}{\rho_l}\right)^{\frac{2}{3}}\left(\frac{1+x}{x}\right)\right]^{-1}$$

(4-4)

The acceleration pressure gradient was estimated as follows:

$$\left(\frac{dp}{dz}\right)_{gravitational} = \left[\frac{(1-x)^2\upsilon_l}{(1-\alpha)} + \frac{x^2\upsilon_g}{\alpha}\right]G^2$$

(4-5)

Table 4-2: Two-phase mixture viscosity models employed in the Homogenous Equation

Author(s)	Equation
McAdams et al. [48]	$\mu_{tp} = \dfrac{1}{\left[\left(\frac{1-x}{\mu l}\right)+\left(\frac{x}{\mu g}\right)\right]^1}$
Akers et al. [29]	$\mu_{tp} = \mu_f[(1-x) + x(\mu_l/\mu_g)]^{-0.5}$
Cicchitti et al. [49]	$\mu_{tp} = (1-x)\mu_l + x\mu_g$
Owens [50]	$\mu_{tp} = \mu_l$
Dukler et al. [51]	$\mu_{tp} = (1-x)\mu_l + x\mu_g$
Beattie and Whalley [52]	$\mu_{tp} = \mu_g\omega + (1-\omega)(1+2.5\omega)\mu_f$
Lin et al. [53]	$\mu_{tp} = \mu_l\mu_g[\mu_g+x^{1.4}(\mu_l-\mu_g)]^{-1}$

4.1 Experimental Results:

- **Effect of mass flux and vapor quality:**

Experimental findings for frictional pressure drop (two-phase) of R152a, R134a, R600a and R1234yf at 27 °C saturation temperature varying mass flux has been visualized in Figure **4.1**. Figure **4.1**(a), shows the behavior of R134a obtained at a different mass flow rate at constant saturation temperature. It has been observed that G= 500 kg/m^{2}s shows maximum pressure drop comparatively at G=400Kg/m^{2}s, G=300 kg/m^{2}s, and G=200 kg/m^{2}s. The result shows that pressure drop increased with the escalation quality and mass flux. Mass flux and velocity that increases the frictional and accelerational inputs of pressure drop, both are directly proportional each other (i.e means increases mass flux eventually increase in pressure drop). At higher vapor quality specific volume increases which is the reason for pressure drop rise along with vapor quality. Figure **4.1**(b,c,d) shows the same trend with different refrigerants.

The same experiment performed at 32 °C saturation temperature has been shown in Figure **4.2**. (a,b,c,d). The outcome shows that the pressure drop was noticed at about 85 percent quality and this was not influenced by difference in mass flux. These predictions are trustworthy and similar to those performed by Gomez et al.[54], Chen et al. [55], Maqbool et al.[4] and Ali et al.[56]
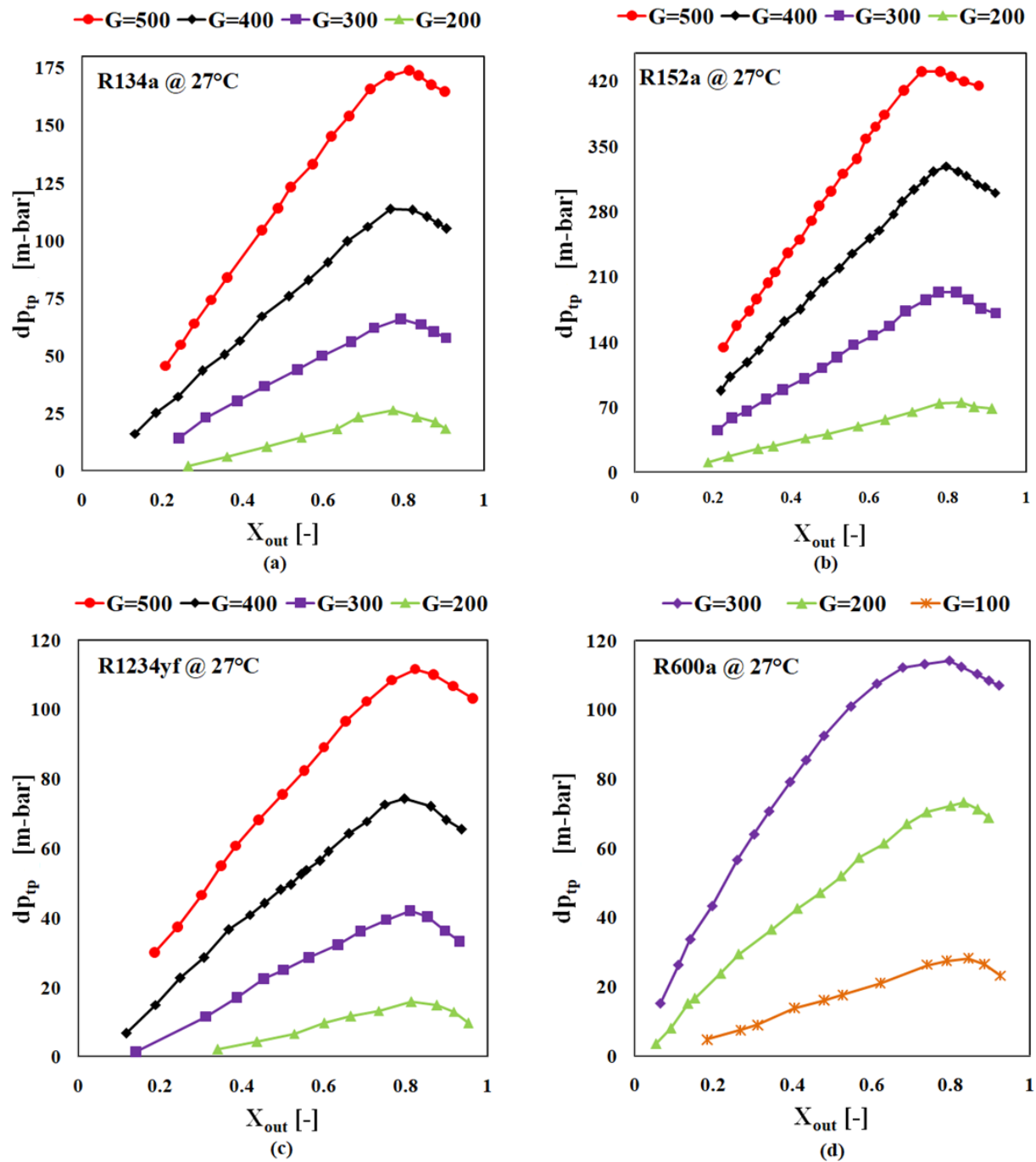
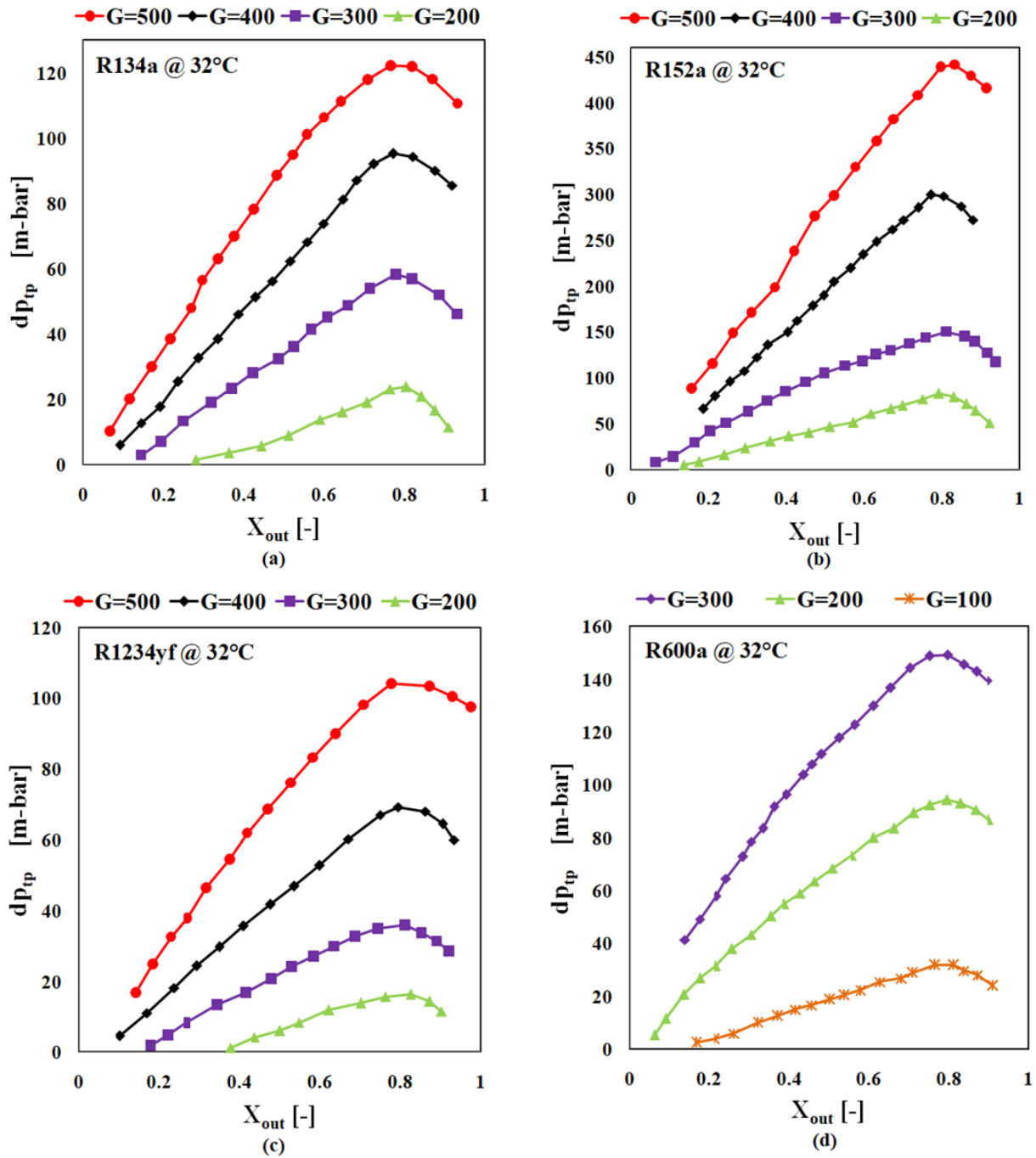Figure 4.1: Effect of mass flux and vapor quality at t_{sat} sat=27°C for (a) R134a, (b) R152a, (c) R1234yf, and (d) R600a

Figure 4.2: Effect of mass-flux and vapor quality at t_sat =32°C for (a) R134a, (b) R152a, (c) R1234yf, and (d) R600a

- **Effect of saturation temperature:**

Consequence of saturation temperature at 32 °C and 27 °C have presented in Figure **4.3**(b). Two-phase frictional pressure drop diminishes with the escalation of saturation temperature from 27 °C to 32 °C for R134yf as a result density of the refrigerant increases and viscosity decreases. It has been observed that different refrigerants show different densities and viscosities for liquid and vapor phases at varying saturating temperatures. At higher saturation temperature outcomes have lesser values of pressure drop. These trends are reliable with those disclosed by Gao et al.[57], Tapia and Ribatski [58] and Del Col et al.[59].

The influence of saturation temperature (27°C) on a two-phase frictional pressure drop has been shown in Figure **4.3**(a). Ethvlidene fluoride and isobutane showed excessive pressure drop than R134a and R1234yf due to their lower vapor density as compare to freon134a and Tetrafluoropropylene. The frictional pressure drop of R1234yf has been observed 33.7 % lower than that of R134a.
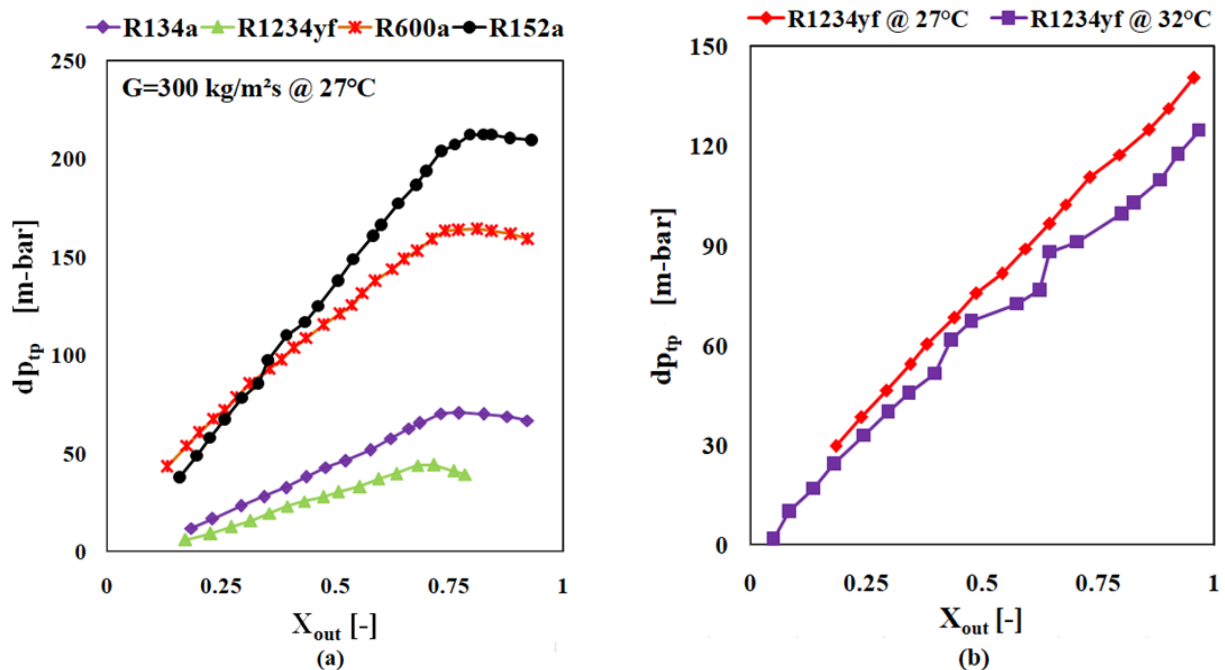

Figure 4.3:(a)Effect of constant temperature using multiple refrigerants at G= 300 kg/m²s, (b) Compare the effect of two-phase frictional pressure drop at different saturation temperature, G=500 kg/m²s using the same refrigerant

- **Effect of heat flux:**

Two-phase frictional pressure drop with mass flux 35 kg/m²s at 32°C and at 27°C have been visualized in Figure **4.4**(a,b). It illustrates that the frictional pressure drop increases with escalation of thermal flux caused by the creation of bubbles near the wall surface of the test conduit. These bubbles collide with each other and with wall surface of the microchannel. The similar results are reported by other authors Chen et al. [55] and Ramírez –Revira et al.[60].
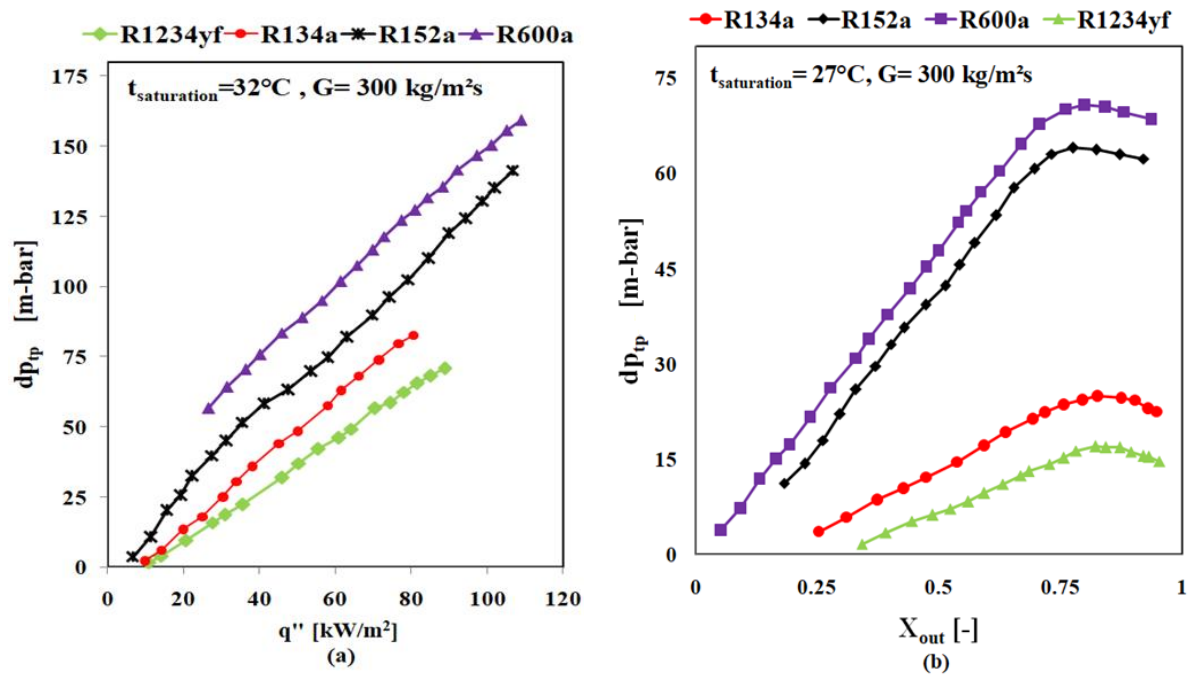
Figure 4.4: Two-phase frictional pressure drop of 1.60 mm tube as a function of heat flux at different saturation temperature

4.2 Comparison with Correlations:

Literature was consulted to compare well known mini/micro correlations for two-phase frictional pressure drop. By splitting the test conduit into ten equal pieces, the pressure gradients were determined. By summing these local gradients, the overall pressure drop was then estimated. In particular, correlations can be distributed into homogenous and separate models for assessing the frictional pressure drop. The homogenous model takes account into flow pattern as single-phase having mean fluid parameters. However, the separated flow model depends on the inputs from

both phases separately with suitable multipliers. For these analysis two different statistical MAE and percentage of data within ±30% was applied. MAE measures the difference between the expected values and the experimental values and is measured as.

$$MAE = \frac{1}{N} \sum_{1}^{N} \left(\frac{x_{predicted} - x_{experimental}}{X_{experimental}} \right) * 100 \qquad \text{(4-6)}$$

A Table **4-3** and Figure **4.5** illustrate the detailed description of comparison and findings.

Thome and Cioncolini [61] presented a novel technique for two-phase flow and observed the relation between liquid film and gas phase using a horizontal channel. The experiment conducted using a vertical and horizontal channel using different diameters from 3 mm to 25 mm. The experimental catalog contains 6290 data points from the literature for 13 different fluids. The findings were compared with Dymel 134a, Isobutane, and Tetarflouropylene and it was observed that data for 1,1-Difluoroethane (percentage data of 30% is 54.12) was under-predicted. The author analyzed the drift-flux model in which relative motion was discussed rather than individual motion of fluid particles. Annular flow and separated two-phase flow cannot be efficiently handled by a drift flux model due to strong dependency on pressure and velocity gradients exiting in two-phase flow.

This model is also an updated version of Lockhart and Martinelli model [62]. Wang conducted experiments using a 6.4 mm horizontal tube with mixture of refrigerants. Fluctuation in mass flux did not effect on the two-phase multiplier. A comparison of our data demonstrated good statistical potential however information for 1,1-Difluoroethane was strongly under-predicted (Figure **4.3**). A possible reason may be the strong dependency of model's two-phase multiplier on mass velocities and physical characteristics of the mixture refrigerant. Thus, the two-phase multiplier for the mixture of refrigerant had considerably lower physical properties than those for pure refrigerants.

Yung and Web published experimental findings for friction pressure drop in a aluminum tube with and without microfin [63]. Pressure gradient escalation with augment the mass velocity and vapor content. The pressure of micro fin conduit was superior to the smooth conduit. Predictive

methods have also been evolved for the both types of flow. These findings indicate that the pressure drop has prevailed in both plain and micro-fin conduits. The comparison shows that R600a is the only refrigerant whose results are up to the mark. A potential justification is surface tension force that effects the frictional pressure drop.

Yu et al [64] examined the phenomena of two-phase pressure drop in a horizontal conduit with a 2.9 mm diameter. Tests were conducted at 200 kPa system pressure and 0.9 m heated length. Experimental findings are viewed as well as comparison with statistical correlations. A transition to Chisholm [65] correlation has been developed in order to better predict small conduit diameter. A comparison of our information with this association demonstrated strong estimates for all examined refrigerants however, under predictions with R152 are clearly visible.

Fourteen refrigerants were used to examined the two phase frictional pressure drop for macro channel [66]. Compare this model with my experimental data shows better performance as shown in Figure **4.5**.

A correlation was proposed by Fridel [28] to quantify the pressure drop in upward flow situation. The experiments conducted using channel diameters from 0.98 to 257.4 mm and operating pressure in the range of 0.06-21 MPa. The experimental databank approximately contains 16000 data points with 13 fluids (R11, R22, R113, water-steam, water-air, oil-air, water-methane, oil-methane, water-nitrogen, alcohol-argon and water-argon). The experiments were conducted for both circular and non-circular conduits. Comparison between our data and the above-mentioned correlation shows amazing results. The result of R152a is under-predicted as shown in Figure **4.5**.

Yan and Lin [67] reviewed experimental findings for pressure drop of natural refrigerants flowing through a small round duct. Analysis of data affects the mass flux, vapor content and thermal flux of natural refrigerant. The author predicted that pressure drop is higher for escalation of mass flux. Comparing our findings with this correlation predict positively. However, our result shows that R600a, R134a under-predict the data while R1234yf predicted the data very well while R152a slightly predict the data.

Belchi [54] given a technique to assessment the two-phase pressure drop phenomena in a tiny-conduit. Experiments were performed in 1.17 mm diameter using multiple refrigerants. Experimental results were quantified to demonstrate the mass velocity, vapor quality and fluid

properties. Compare this correlation with our data shoes better performance as shown in Figure 4.5

(a)

(b)

(c)

(d)
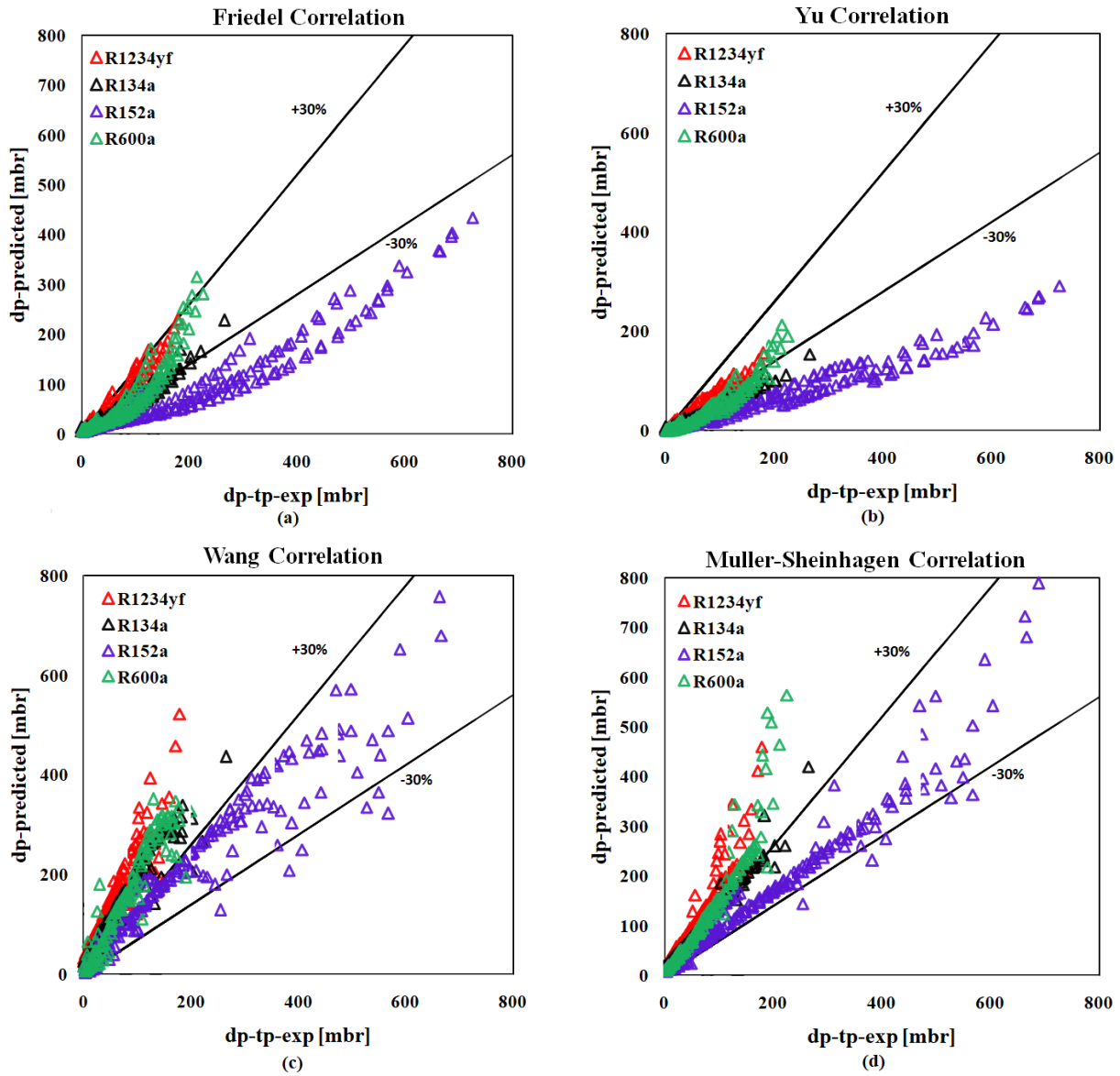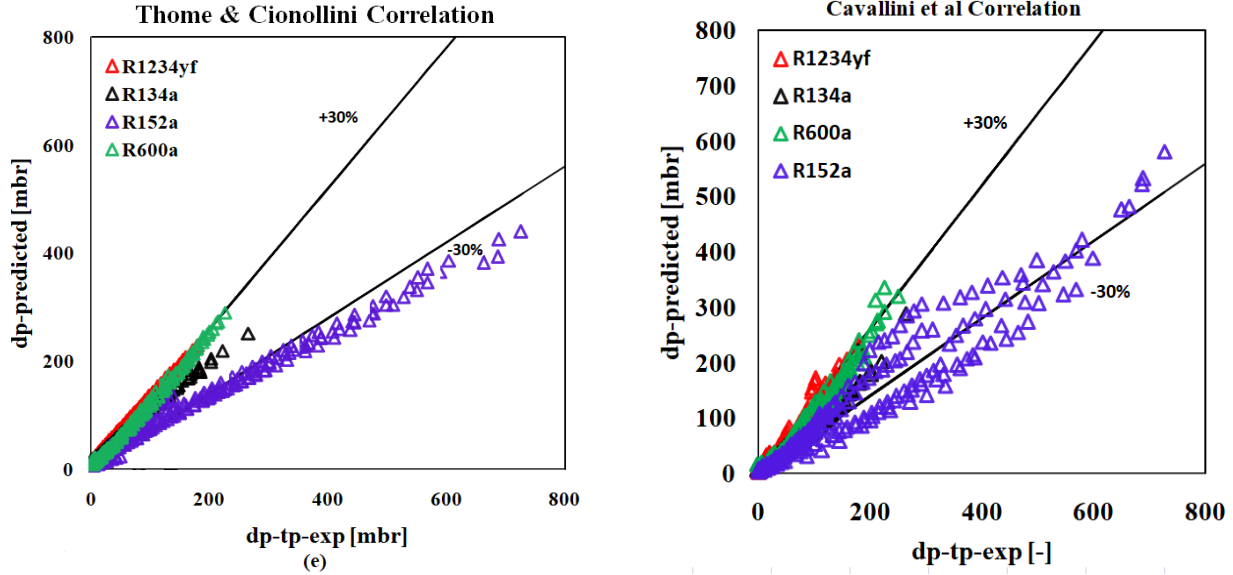
Figure 4.5: Comparison of frictional pressure drop trends according to predictive and experimental data (a)Friedel correlation (b)Yu correlation (c)Wang correlation (d)Muller-Sheinhagen correlation (e)Thome & Cionollini correlation (f)Cavallini et al correlation

4.3 New Proposed correlation:

Cavalline et al. predicted two-phase frictional pressure drop which is shown as followed:

$$\left(\frac{dp}{dz}\right)_{tp} = \emptyset^2{}_{lo}\left(\frac{dp}{dz}\right)_{lo} = \emptyset^2{}_{lo} 2 * f'_{LO}\frac{G^2}{D_h\rho_L} \tag{4-7}$$

Where friction factor (f') refered to surface roughness and (f'_{LO}) demonstrated the Reynold number. Eq.(**4-9**) gives us two-phase multiplier like a part of vapor content, entrained liquid fraction E and the reduced pressure. Entrained liquid fraction can be explained as the liquid flow fraction in terms of droplets in gaseous phase. Total mass flow consists of three different characteristics of annular flow considering entrained liquid fraction and quality. Pressure drop and dry-out in the flow region can be estimated by its prediction. Virtual increase in the density of vapor phase reduced the pressure due to the entrained liquid in gaseous phase. Hewitt and Hall-Taylor [68] Paleev and Filippovich [69] suggested the entrainment ration in Eq.(**4-10**) to be calculated.

$$\rho'_{LO} = 0.046Re^{-0.2}{}_{LO} \tag{4-8}$$

45

$$\varnothing^2{}_{lo} = 3.595 * F * H * (1 - E)^W + Z \tag{4-9}$$

$$E = 0.44\log\left[\left(\frac{\rho_{GC}}{\rho_L}\right) * \left(\frac{\mu_{jG}}{\sigma}\right)^2 * 10^4\right] + 0.015 \tag{4-10}$$

$$W = 1.398P_R \tag{4-11}$$

$$Z = (1 - x)^2 + x^2 * \frac{\rho_L}{\rho_G}\left(\frac{\mu_G}{\mu_L}\right)^{0.2} \tag{4-12}$$

$$H = \left(\frac{\mu_g}{\mu_L}\right)^{0.44}\left(\frac{\rho_l}{\rho_g}\right)^{1.132}\left(1 - \frac{\mu_G}{\mu_L}\right)^{3.542} \tag{4-13}$$

Multiple regression analysis was used to modify the (Cavallini et al. [70]) correlation. More variation in experimental data was observed as compared to the predicted data when flow boiling frictional pressure drop for all four refrigerants (HFC-R134a, Isobutane, Ethylidene fluride and Tetrafluoropylene) were compared. Therefore, comparison of our experimental data (Figure **4.6**) with correlation showed good predictions, modified equation (Fig (4-14)) predicted the 71.87 % of data within ±30 range.

$$F = \frac{x^{0.9525} * (1 - x)^{0.414}}{3.25} \tag{4-14}$$
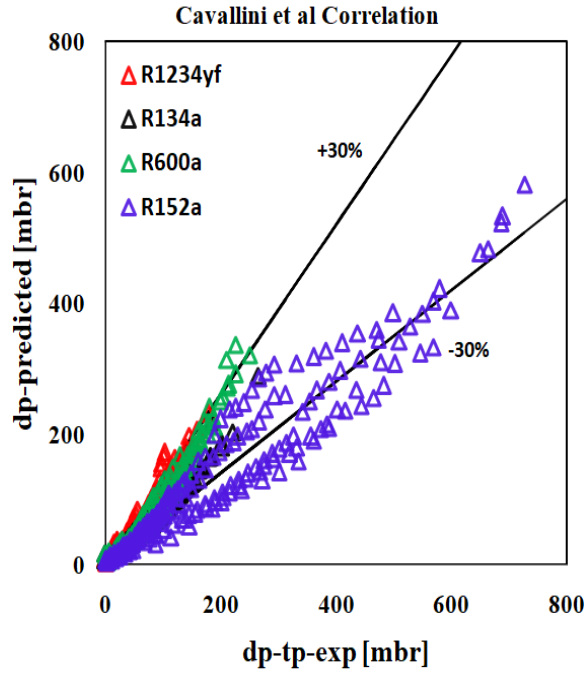
Figure 4.6 Comparison of experimental data with newly proposed correlation

Table 4-3: Outline of important statistical data about the tested correlations

Correlation	MAE	Percentage of data within ±30%
Thome & Cionolini [18]	27.08	54.12
Belchi [60]	23.45	29.20
Cavallini [70]	27.24	71.78
Sun and Mishima [71]	39.44	33.02
Yang and Web [63]	46.78	29.04
Yu [64]	42.19	26.63
Mishima [72]	24.04	30.95
Wang [62]	34.36	53.55
Muller-Steinhagen [66]	40.71	27.55
Tran et al [73]	45.23	47.62
Lockhart & Martinelli [74]	52.36	42.49
Hwang and Kim [75]	55.67	39.63

Friedel [28]	34.59	37.01
Li and Wu [20]	41.74	37.01
Jung & Radermacher [76]	33.33	46.41
Grönnerud [77]	30.77	52.05

Chapter 5 Conclusion and Future Recommendation:

5.1 Conclusion:

Experimental findings on frictional pressure drop of pure refrigerants (HFC-134a, Isobutane, Difluoroethane and Tetrafluoropropylene) in vertical mini/microchannel were presented in this thesis. The key findings are;

- The Frictional pressure drop improved with the escalation of the mass flux and vapor content. Mass flux and velocity that increases the frictional and acceleration inputs of pressure drop are directly proportional, means increases mass flux eventually surge in pressure drop.

- R152a and R600a demonstrate superior results than R134a and R1234yf and consequence can be clarified by the dissimilarity in thermo-physical characteristics.

- The consequences of higher saturation temperature results in a lesser value of frictional pressure drop owing to diminish the vapor velocity and liquid viscosity.

- The two-phase frictional pressure drop increases with the escalation of heat flux. Because the formations of bubbles near the tube surface get bigger with the escalation of heat flux.

- Twenty exiting frictional pressure drop models have been associated with the experimental data of multiple refrigerants including HFC-134a, Isobutane, Difluoroethane and Tetrafluoropropylene. The updated version of Cavallini et al. showed best predictions with 71.78 % of data within ±30% band error.

The pressure drop peak was noticed at approximately 85% vapor content in all situations, and this was not affected by the change in mass flux.

5.2 Future Recommendation:

The fluid flow channel size is becoming smaller and smaller. The use of micro and mini channel heat exchangers is undoubtedly increased in air conditioning applicants owing to its favorable characteristics like higher heat and mass transfer, compact system, lightweight, and lower cost, etc. The mini channel uses less power and refrigerant charge so it is also good for the environment. In addition, more and more microchannel heat exchangers have been used for commercial and household products.

This research did not concentrate on any particular purpose. Particular applications of heating and cooling were focused during performing of experiments so that components used become more affective. Infrared thermometry is a modern and quick simulation analysis technique which can be helpful in selecting transition limits for different flow patterns.

It is also necessary to test a wider spectrum range of working circumstances (system pressure, inlet conditions, conduit arrangement, and properties)

References:

[1]   S. H. Lee and I. Mudawar, "Investigation of flow boiling in large micro-channel heat exchangers in a refrigeration loop for space applications," Int. J. Heat Mass Transf., vol. 97, pp. 110–129, 2016.

[2]   A. P. Roday and M. K. Jensen, "A review of the critical heat flux condition in mini-and microchannels," J. Mech. Sci. Technol., vol. 23, no. 9, pp. 2529–2547, 2009.

[3]   R. Ali and B. Palm, "Dryout characteristics during flow boiling of R134a in vertical circular minichannels," Int. J. Heat Mass Transf., vol. 54, no. 11–12, pp. 2434–2445, 2011.

[4]   M. H. Maqbool, B. Palm, and R. Khodabandeh, "Experimental investigation of dryout of propane in uniformly heated single vertical mini-channels," Exp. Therm. Fluid Sci., vol. 37, pp. 121–129, 2012.

[5]   J. E. Aldy and R. N. Stavins, "Climate Negotiators create an Opportunity for Scholars," 2012.

[6]   S. O. Andersen, D. Brack, and J. Depledge, "A Global Response to HFCs through Fair and Effective Ozone and Climate Policies," Energy, Environ. Resour., no. July, pp. 1–48, 2014.

[7]   M. O. McLinden, J. S. Brown, R. Brignoli, A. F. Kazakov, and P. A. Domanski, "Limited options for low-global-warming-potential refrigerants," Nat. Commun., vol. 8, pp. 1–9, 2017.

[8]   S. O. Andersen, M. L. Halberstadt, and N. Borgford-Parnell, "Stratospheric ozone, global warming, and the principle of unintended consequences-An ongoing science and policy success story," J. Air Waste Manag. Assoc., vol. 63, no. 6, pp. 607–647, 2013.

[9]   R. Grönnerud, "Investigation of liquid hold-up, flow resistance and heat transfer in

circulation type evaporators, Part IV: Two phase flow resistance in boiling," J. Enviromental Mnagement, 1979.

[10] C. Of et al., "Report of the conference of the parties on its third session, held at Kyoto," pp. 1–60, 1998.

[11] J.H.KOH and Z.ZAKARIA, "Hydrocarbons as Refrigerants—A Review," ASEAN J. Sci. Technol. Dev., vol. 34, no. 1, p. 35, 2017.

[12] S. G. Kandlikar, S. Garimella, L.Dongqing, S. Colin, and M. R.King, Heat transfer and fluif flow in minichannels and microchannels. .

[13] S.Kandlikar and W.J.Grande, "Evolution of microchannel flow passages-thermohydraulic performance and fabrication technology," Heat Transf. Eng., no. May 2012, pp. 37–41, 2010.

[14] S. S. Mehendafe and A. M. Jacob, "Fluid flow and heat transfer at micro- and meso-scales with application to heat exchanger design *," Am. Socity Mech. Eng., vol. 53, no. 7, 2016.

[15] S. G. Kandlikar and W. J. Grande, "Evaluation of microchannel flow passages," pp. 1–13, 2002.

[16] P. A. Kew, "Correlation for the prediction heat transfer in single-diameter of boiling," Appl. Therm. Eng., vol. 17, pp. 705–715, 1997.

[17] K.A.Triplett, S.M.Ghiaasiaan, and D.L.Sadowski, "Gas-liquid two-phase flow in microchannels Part I : two-phase flow patterns," Int. J. Multiph. Flow, vol. 25, pp. 377–394, 1999.

[18] C. L. Ong and J. R. Thome, "Macro-to-microchannel transition in two-phase flow : Part 1 – Two-phase flow patterns and film thickness measurements," Exp. Therm. Fluid Sci., vol. 35, no. 1, pp. 37–47, 2011.

[19] T. Harirchian and S. V Garimella, "A comprehensive flow regime map for microchannel flow boiling with quantitative transition criteria," Int. J. Heat Mass Transf., vol. 53, no. 13–14, pp. 2694–2702, 2010.

[20]   W. Li and Z. Wu, "A general criterion for evaporative heat transfer in micro / mini-channels," Int. J. Heat Mass Transf., vol. 53, no. 9–10, pp. 1967–1976, 2010.

[21]   Incropera, Dewitt, Bergman, and Lavine, Fundamentals of heat and mass transfer, Sixth edit.

[22]   G.Ribatski, L.Wojtan, and J.R.Thome, "An analysis of experimental data and prediction methods for two-phase frictional pressure drop and flow boiling heat transfer in micro-scale channels," Exp. Therm. Fluid Sci., pp. 1–19, 2006.

[23]   L.G.Heat and F.Mitigation, "Compact heat exchangers for energy transfer intensification low grade heat anf fouling mitigation," Int. Commun. Heat Mass Transf.

[24]   J.Judy, D.Maynes, and B.W.Webb, "Characterization of frictional pressure drop for liquid flows through microchannels," Int. J. Heat Mass Transf., vol. 45, no. 17, pp. 3477–3489, 2002.

[25]   B. A. Shannak, "Frictional pressure drop of gas liquid two-phase flow in pipes," Nucl. Eng. Des., vol. 238, no. 12, pp. 3277–3284, 2008.

[26]   S. Kim and I. Mudawar, "Universal approach to predicting two-phase frictional pressure drop for adiabatic and condensing mini / micro-channel flows," Int. J. Heat Mass Transf., vol. 55, no. 11–12, pp. 3246–3261, 2012.

[27]   G. A. Longo, S. Mancin, G. Righetti, and C. Zilio, "Saturated vapour condensation of R134a inside a 4 mm ID horizontal smooth tube: Comparison with the low GWP substitutes R152a, R1234yf and R1234ze(E)," Int. J. Heat Mass Transf., vol. 133, pp. 461–473, 2019.

[28]   L, Friedel, "Improved friction pressure drop correlations for horizontal and vertical two phase pipe flow," Eur. Two-phase Meet. Ispra-Italy, vol. 25, 1979.

[29]   W.W.Akers, H. A. Deans, and O. K. Crosser, "Condensing heat transfer within horizontal tubes," Chem. Eng. Prog., pp. 89–90, 1958.

[30]   S. Novianto, A. S. Pamitran, R. Koerstoer, and K. Saito, "Two-phase Frictional Pressure

Drop of Propane with Prediction Methods of Viscosity and Density in 500 μm Diameter Tube," Mater. Sci. Eng., 2018.

[31]   K. Choi, A. S. Pamitran, J. Oh, and K. Saito, "Pressure drop and heat transfer during two-phase flow vaporization of propane in horizontal smooth minichannels," Int. J. Refrig., vol. 32, no. 5, pp. 837–845, 2009.

[32]   X. Li and T. Hibiki, "Frictional pressure drop correlation for two-phase flows in mini and micro single-channels," Int. J. Multiph. Flow, vol. 90, pp. 29–45, 2017.

[33]   N. Liu, J. M. Li, J. Sun, and H. S. Wang, "Heat transfer and pressure drop during condensation of R152a in circular and square microchannels," Exp. Therm. Fluid Sci., vol. 47, pp. 60–67, 2013.

[34]   D. R. E. Ewim and J. P. Meyer, "Pressure drop during condensation at low mass fluxes in smooth horizontal and inclined tubes," Int. J. Heat Mass Transf., vol. 133, pp. 686–701, 2019.

[35]   M. Hirose, J. Ichinose, and N. Inoue, "Development of the general correlation for condensation heat transfer and pressure drop inside horizontal 4 mm small-diameter smooth and microfin tubes," Int. J. Refrig., vol. 90, pp. 238–248, 2018.

[36]   D. Jige, N. Inoue, and S. Koyama, "Condensation of refrigerants in a multiport tube with rectangular minichannels," Int. J. Refrig., 2016.

[37]   M. H. Maqbool, B. Palm, and R. Khodabandeh, "Investigation of two phase heat transfer and pressure drop of propane in a vertical circular minichannel," Exp. Therm. Fluid Sci., vol. 46, pp. 120–130, 2013.

[38]   A. M. Md.Anowar Hossain, Hasan MM Afroz, "Two-phase frictional multipiler correlation for the prediction of condensation pressure drop inside smooth horizontal tube," 6th BSME Int. Conf. Therm. Eng., vol. 105, no. Icte 2014, pp. 64–72, 2015.

[39]   Y. Xu and X. Fang, "A new correlation of two-phase frictional pressure drop for condensing flow in pipes," Nucl. Eng. Des., vol. 263, pp. 87–96, 2013.

[40] S. Saisorn and S. Wongwises, "The effects of channel diameter on flow pattern , void fraction and pressure drop of two-phase air – water flow in circular micro-channels," Exp. Therm. Fluid Sci., vol. 34, no. 4, pp. 454–462, 2010.

[41] W. Owhaib, Experimental Heat Transfer , Pressure Drop , and Flow Visualization of R-134a in Vertical Mini / Micro Tubes, no. 07. 2007.

[42] M. H. Maqbool, B. Palm, and R. Khodabandeh, "International Journal of Thermal Sciences Boiling heat transfer of ammonia in vertical smooth mini channels : Experimental results and predictions," Int. J. Therm. Sci., vol. 54, pp. 13–21, 2012.

[43] R. Khodabandeh, "Flow Boiling Heat Transfer and Dryout Characteristics of R600a in a Vertical Minichannel," Heat Transf. Eng., vol. 36, pp. 1230–1240, 2015.

[44] Z. Anwar, B. Palm, and R. Khodabandeh, "Flow boiling heat transfer , pressure drop and dryout characteristics of R1234yf : Experimental results and predictions," Exp. Therm. FLUID Sci., vol. 66, pp. 137–149, 2015.

[45] Z. Anwar and T. Lahore, "Evaporative Heat Transfer with R134a in a Vertical Minichannel," Pak.J.Engg. & Appl.Sci, vol. 13, pp. 101–109, 2013.

[46] J. Y. Yun and K. S. Lee, "Influence of design parameters on the heat transfer and flow friction characteristics of the heat exchanger with slit fins," Int. J. Heat Mass Transf., vol. 43, no. 14, pp. 2529–2539, 2000.

[47] M. H. Maqbool, B. Palm, and R. Khodabandeh, "Flow boiling of ammonia in vertical small diameter tubes : Two phase frictional pressure drop results and assessment of prediction methods," Int. J. Therm. Sci., vol. 54, pp. 1–12, 2012.

[48] W. H. McAdams, W. k. Woods, and L. C. Heroman, "Vaporization inside horizontal tubes – II: Benzene–oil mixture, Trans.," Ind. Eng. Chem., vol. 41, pp. 193–200, 1942.

[49] A. Cicchitti, C. Lombardi, M. Silvestri, G. Soldaini, and R. Zavalluilli, "Two-phase cooling experiments-pressure drop, heat transfer and burnout measurements," JACC Cardiovasc. Interv., pp. 407–425, 1960.

[50] W. L. Owens, "Two-phase pressure gradient, Int. Dev. Heat Transfer, Pt. II," ASME,New York, 1961.

[51] A. E. Dukler, M. Wicks, and R. G. Clwaveland, "Pressure drop and hold up in twophase flow," Int. J. Multiph. Flow, pp. 38–51, 1964.

[52] D. R. H. Beattie and P. B. Whalley, "A simple two-phase frictional pressure drop calculation method," Int. J. Multiph. Flow, pp. 83–87, 1982.

[53] S. Lin, C. C. K. Kwok, R. Y. Li, Z. H. Chen, and Z. Y. Chen, "S. Lin, C.C.K. Kwok, R.Y. Li, Z.H. Chen, Z.Y. Chen, Local frictional pressure drop during vaporization of R-12 through capillary tubes," Int. J. Multiph. Flow, pp. 95–102, 1991.

[54] A. López-belchí, F. Illán-gómez, F. Vera-garcía, and J. R. García-cascales, "Experimental condensing two-phase frictional pressure drop inside mini-channels . Comparisons and new model development," Int. J. Heat Mass Transf., vol. 75, pp. 581–591, 2014.

[55] X. Chen, S. Chen, J. Chen, J. Li, X. Liu, and L. Chen, "Two-phase flow boiling frictional pressure drop of liquid nitrogen in horizontal circular mini-tubes : Experimental investigation and comparison with correlations," Cryogenics (Guildf)., 2017.

[56] R. Ali, B. Palm, and M. H. Maqbool, "Experimental investigation of two-phase pressure drop in a microchannel," Heat Transf. Eng., vol. 32, no. 13–14, pp. 1126–1138, 2011.

[57] Y. Gao, Y. Feng, S. Shao, and C. Tian, "Two-phase pressure drop of ammonia in horizontal small diameter tubes: Experiments and correlation," Int. J. Refrig., 2018.

[58] D. F. Sempértegui-tapia, G. Ribatski, H. Transfer, E. De Engenharia, D. S. Carlos, and S. Paulo, "Two-phase frictional pressure drop in horizontal micro-scale channels : Experimental data analysis and prediction method development," Int. J. Refrig., vol. 79, pp. 143–163, 2017.

[59] D. Del Col, D. Torresin, A. Cavallini, V. Venezia, and F. Tecnica, "Heat transfer and pressure drop during condensation of the low GWP refrigerant R1234yf Transfert de chaleur et chute de pression lors de la ` ne R1234yf dote ´ d ' un faible condensation du frigorige ´ chauffement plane ´ taire potentiel de re," Int. J. Refrig., vol. 33, no. 7, pp.

1307–1318, 2010.

[60] F. Vera-García, F. Illán-Gómez, A. López-Belchí, F. Ramírez-Rivera, and J. R. García-Cascales, "Two phase flow pressure drop in multiport mini-channel tubes using R134a and R32 as working fluids," Int. J. Therm. Sci., vol. 92, pp. 17–33, 2015.

[61] A. Cioncolini and J. R. Thome, "Improved friction pressure drop correlations for horizontal and vertical two phase pipe flow," Int. J. Multiph. Flow, 2016.

[62] C. Wang and D. Lu, "Visual Observation of Two-Phase Flow Pattern of R-22, R-134a, and R-407C in a 6.5 mm smooth tube," Elsevier, vol. 1777, no. 97, pp. 395–405, 1997.

[63] C. Yang and R. L. Webbt, "Friction pressure drop of R-12 in small hydraulic diameter extruded aluminum tubes with and without micro-fins," Int. J. Heat Mass Transf., vol. 39, no. 4, 1996.

[64] W. Yu and D. M. France, "Two-phase pressure drop , boiling heat transfer , and critical heat flux to water in a small-diameter horizontal tube," Int. J. Mult. Flow, vol. 28, pp. 927–941, 2002.

[65] D. Chisholm, "Pressure gradients due to friction during the flow of evaporating two-phase mixtures in smooth tubes and channels," Int. J. Heat Mass Transf., vol. 16, no. 29, pp. 347–358, 1973.

[66] H. M. Steinhagen and K. Heck, "A Simple Friction Pressure Drop Correlation for Two-Phase Flow in Pipes," Chem. Eng. Prog., vol. 20, no. 1, pp. 297–308, 1986.

[67] Y. Yan and F. Lin, "Evaporation heat transfer and pressure drop of refrigerant R!023a in a small pipe," Int. J. Heat Mass Transf., 1998.

[68] N. Hall Taylor, G. F. Hewitt, and P. M. C. Lacey, "The motion and frequency of large disturbance waves in annular two-phase flow of air-water mixtures," Chem. Eng. Sci., vol. 18, no. 8, pp. 537–552, 1963.

[69] I. I. Paleev and B. S. Filippovich, "Phenomena of liquid transfer in two-phase dispersed annular flow," Int. J. Heat Mass Transf., vol. 9, no. 10, pp. 1089–1093, 1966.

[70] A. Cavallini, D. Del Col, M. Matkovic, and L. Rossetto, "Fluid Flow Frictional pressure drop during vapour – liquid flow in minichannels : Modelling and experimental evaluation," Int. J. Heat Fluid Flow, vol. 30, pp. 131–139, 2009.

[71] L. Sun and K. Mishima, "Flow Evaluation analysis of prediction methods for two-phase flow pressure drop in mini-channels d," Int. J. Multiph. Flow, vol. 35, no. 1, pp. 47–54, 2009.

[72] K. Mishima and T. Hibiki, "Some characteristics of air-water two-phase flow in small diameter vertical tubes," Int. J. Multiph. Flow, vol. 22, no. 4, pp. 703–712, 1996.

[73] T. N. Tran, M. C. Chyu, M. W. Wambsganss, and D. M. France, "Two-phase pressure drop of refrigerants during flow boiling in small channels: An experimental investigation and correlation development," Int. J. Multiph. Flow, vol. 26, no. 11, pp. 1739–1754, 2000.

[74] L. R. . and M. R.C, "Proposed correlation of data for isothermal two-phase, two-phase component flow in pipes." .

[75] Y. Hwang and M. S. Kim, "The pressure drop in microtubes and the correlation development," Int. J. Heat Mass Transf., vol. 49, pp. 1804–1812, 2006.

[76] D. S. Jung and R. Radermacher, "Prediction of pressure drop during horizontal annular flow boiling of pure and mixed refrigerants," Int. J. Heat Mass Transf., vol. 32, no. 12, pp. 2435–2446, 1989.

[77] R. Grönnerud, "Investigation of liquid hold-up, flow resistance and heat transfer in circulation type evaporators, Part IV: Two phase flow resistance in boiling," Energy Concersion Manag., 1979.